

Report No. 6/1993 vol. 7

J. Hyttinen and J. Malmivuo (eds.)

**Proceedings of the Second Ragnar Granit
Symposium: EEG and MEG Signal Analysis and
Interpretation,
November 22-23, 1993,**

Tampere, 1993



Tampere University of Technology

RAGNAR GRANIT INSTITUTE

**Proceedings of the Second Ragnar Granit Symposium:
EEG and MEG Signal Analysis and Interpretation,
November 22-23, 1993**

Organized by
Ragnar Granit Institute
and
Finnish Society for Medical Physics and Medical Engineering

J. Hyttinen and J. Malmivuo (eds.)

Report No. 6/1993 vol. 7

ISBN 951-722-076-6
ISSN 1235-8800

Contents

| | |
|-------------------------------------------------------------------------------------------------------------------------------------------------------------------------------|----|
| Foreword | 1 |
| Sources of the EEG and MEG Signals | 2 |
| EEG as a Reflection of Brain Functions; Sources and Analysis (Prof. F.H. Lopes da Silva) | 3 |
| From EEG Source Localization to Source Imaging (Prof. Michael Scherg) | 6 |
| Source Analysis of the Brain's Electromagnetic Signals (Dr. Tech. Matti Hämäläinen) | 8 |
| Higher Brain Functions Reflected in MEG (Docent Mikko Sams) | 9 |
| Reactivity of the Spontaneous MEG Activity (Dr. Tech. Riitta Salmelin) .. | 10 |
| Half-Sensitivity Volumes in EEG and MEG Measurements (M.Sc. Veikko Suihko and prof. Jaakko Malmivuo) | 11 |
| Signal Analysis | 21 |
| The Integration of EEG, MEG, and Magnetic Resonance Images (Ph.D. Simon Walker) | 22 |
| Applying an Average Mutual Information Based Multivariate Autoregressive Model to Describe Correlated Noise Sources of EEG in Anesthesia (Lic. Tech. Pekka Loula) | 27 |
| ABR Signal as a Digital Signal (M.Sc. Tapani Grönfors) | 33 |
| Signal Interpretation | 36 |
| Dynamical Aspects of Magnetic Source Imaging (Prof. Samuel Williamson) .. | 37 |
| Event Related Desynchronous Registration (Ph.D. Kalervo Suominen) | 41 |
| Patterns and Topology of Burst Suppression (Docent Ville Jäntti) | 43 |
| EEG and ERP Dynamics in Slight Vigilance Variations (M.D. Hannu Mikola) | 46 |
| Electrophysiological Changes in Reduced Vigilance (Docent Joel Hasan) .. | 47 |
| Appendix | 51 |
| List of Symposium Participants | 52 |

Foreword

The recent development in MEG and EEG source localization and signal analysis methods has been swift. Technical improvements have been particularly fast in magnetic measurements of brain functions. These noninvasive methods to appraise brain functions have been more widely combined with imaging methods and volume conductor modelling. New terms such as source imaging has been introduced when attaining the source characteristics. The assessment of brain function from the complexity of spontaneous signals is more a matter of signal analysis and interpretation methods. This symposium compiles the state of the art of Finnish and international research of the brain electromagnetic activity including source analysis and signal analysis and interpretation.

I would like to thank our invited international lecturers; Professors F.H. Lopes da Silva, Michael Scherg and Samuel Williamson for participating the seminar. These acknowledged researchers have conducted active research both in source identification and in signal analysis. Their contributions form the solid framework of the symposium. The wide range of subjects in this symposium reflect the strength of Finnish research in this field. All the major universities are introducing their special knowledge to the field indicating the wide basis of brain research in our country.

This symposium bears the name "Second Ragnar Granit symposium" honoring the name of the Finnish-Swedish Nobel laureate Ragnar Granit. Ragnar Granit Institute of Tampere University of Technology hosts the symposium and welcomes all the lecturers and participants. The symposium is organized in association with the Finnish Society of Medical Physics and Medical Engineering

The program of the symposium was organized by a committee, whose members are Prof. Riitta Hari, prof. Heikki Lang, prof. Uolevi Tolonen, docent Ville Jäntti, docent Hannu Eskola, docent Pekka Karp (chairman of the society) and lic. tech. Jari Hyttinen (secretary of the society). Their work has been of great importance for the success of the seminar.

I wish to express my gratitude to Soile Lönnqvist, the secretary of the symposium and the staff of the Ragnar Granit Institute for their help in the practical arrangement of the symposium. The symposium is supported by the Academy of Finland and the City of Tampere. Their support is gratefully acknowledged.

Sources of the EEG and MEG Signals

EEG/MEG as a Reflection of Brain Functions: Sources and Analysis

Fernando H. Lopes da Silva

Graduate School for Neurosciences, Institute of Neurobiology

Faculty of Biology, University of Amsterdam, Kruislaan 320, 1098 SM

The Netherlands

The scalp EEG/MEG reflects mainly the activity of the neuronal populations at the surface of the brain hemispheres, namely at the cortex. A basic question is whether the activity of these neuronal populations as revealed in the EEG/MEG can be related in a clear way to well defined brain functions, or whether it must be considered a simple epiphenomenon. In order to answer this question, it is necessary to have an understanding of the biophysical principles underlying EEG/MEG signals. The objective of this brief overview is to analyse a number of current issues that are important in order to improve our understanding of the significance of on-going EEG/MEG signals. EEG/MEG signals are detectable at the surface of the scalp when the amount of synchrony of the neuronal population activity reaches a sufficient level. The occurrence of oscillations play a main role in promoting this synchrony. In more general terms, it is necessary to take into consideration the dynamics of these neuronal populations and how this can be reflected in the EEG/MEG signals.

The establishment of assemblies of neurons exhibiting correlated activity depends primarily on the connectivity of the neurons within networks. In general, the neurons are interconnected by means of feedforward and feedback connections, namely excitatory and inhibitory synaptic connections. An example is the case of the alpha rhythm of the visual cortex. A system of interconnections assures the spread of alpha activity over several millimetres distance. However, other brain rhythmic activities, as for example some types of beta rhythmic activity, may be generated in more restricted cortical areas.

The occurrence of oscillations in a neuronal population usually implies a relatively large degree of synchrony between the neurons. In this way, the formation of areas of correlated activity is likely to be enhanced. A basic question is whether the oscillations depend on intrinsic membrane properties of the "pacemaker" type, or on synaptic feedback circuits with time delays, or both. In this respect, the best studied system is the thalamic nuclei where spindles at different frequencies, including the alpha band, can occur. The thalamic neurons can work essentially in distinct modes, depending on initial conditions, i.e. on the level of the corresponding membrane potential: as generators of single spikes or as oscillatory cells producing bursts of spikes that are repeated rhythmically. Furthermore, in the latter mode they may oscillate at different frequencies. The frequency of oscillation depends on the three types of factors: - the intrinsic membrane properties of neurons, - the initial level of the membrane potential that, in turn, can be modulated by a number of input systems, and - the strength of the synaptic interactions. Chemical neuromodulatory systems are important to regulate the set-points of different neuronal populations, and in this way, to enable these to switch between different oscillatory modes. Feedback synaptic inhibition is also an efficient mechanism to enhance the synchrony within neuronal populations since the axons of

inhibitory interneurons usually ramify profusely, and the corresponding synapses occupy strategically paced sites at the soma and near to the initial segments of axons of the pyramidal neurons.

A question of current debate is whether neuronal networks can have multiple attractors and exhibit bifurcations to chaotic oscillations. That this is likely is not unexpected if we take into account that the behaviour of such networks can be described by systems of coupled non-linear differential equations with time delays. Such networks can exhibit different modes of behavior that can be described by different types of attractors. Under some circumstances, namely at the transition from a resting on-going EEG to an epileptic seizure a state bifurcation, in the dynamics of the neuronal population, from a random state (very high dimension) to one characterized by a chaotic attractor of low dimension can take place. The bifurcation to a state characterized by chaotic oscillations may also play an important role in enhancing the synchrony of neuronal populations since, under these conditions, the oscillations tend to propagate throughout the cortex or even the whole brain. However, this is a pathological state and these oscillations will disrupt the normal functioning of the brain.

In conclusion, we can state that neuronal assemblies with a high degree of internal correlation, between the cellular elements, occur in the brain. Under normal conditions, a relatively large number of distinct assemblies are simultaneously active. This is reflected in the EEG/MEG signals recorded in the alert state that exhibit a large number of degrees of freedom and non-stationarity. The existence of coherent assemblies of neurons, forming a distributed system, may be important for the encoding of sensory and motor information, and, more in general, for the functional organization of the brain (gating functions, synaptic plasticity). However, under conditions of reduced consciousness, or alertness, the dynamics change into a state characterized by a low-dimensional chaotic attractor.

SELECTED OWN REFERENCES

De Munck, J.C., Vijn, P.C.M. and Lopes da Silva, F.H. A Random dipole model for spontaneous brain activity. IEEE Biomed. Eng., , 1992, 39: 791-804.

Fernandes de Lima, V.M., Pijn, J.P., Filipe, C.N. and Lopes da Silva, F.H. The role of hippocampal commissures in the interhemispheric transfer of epileptiform afterdischarges in the rat: a study using linear and non-linear regression analysis. *Electroencephalor. Clin. Neurophysiol.* 1990, 76: 520-539

Lopes da Silva, F.H., Vos, J.E., Mooibroek, j. and van Rotterdam, A. Reallive contributions of intracortical and thalamo-cortical processes in the generation of alpha rhythms, revealed by partial coherence analysis. *Electroenceph. Clin. Neurophysiol.*, 1980, 50: 449-456.

Lopes da Silva, F.H., van Rotterdam, A., Storm van Leeuwen, W. and Tielen, A.M. Dynamic characteristics of visual evoked potentials in the dog. II. Beta frequency selectivity in evoked potentials and background activity. *Electroenceph. Clin. Neurophysiol.*, 1970, 29: 260-268.

Pijn, J.P., Van Neerven, J., Noest, A. and Lopes da Silva, F.H. Chaos or noise in EEG signals; dependence on state and brain site. *Electroenceph. Clin. Neurophysiol.*, 1991, 79: 371-381.

Rotterdam, A. van, Lopes da Silva, F.H., van den Ende, J., Viergever, M.A. and Hermans, A.J. A model of the spatial-temporal characteristics of the alpha rhythm. *Bull. of Mathem. Biol.*, 1982, 44: 283-305.

Lopes da Silva, F.H., Hoeks, A., van Lierop, T.H.M.T., Schijer, C.F.M. and Storm van Leeuwen, W. Confidence limits of spectra and coherence functions - Their relevance for quantifying thalamo-cortical relationships of alpha rhythms. In: *Die Quantifizierung des Elektroenzephalogramms* (Ed. G.K. Schenk), AEG Telefunken, Konstanz, 1973, 437-449.

Steriade, M. Gloor, Pl, Llinás, R.R., Lopes da Silva, F.H. and Mesulam, M. Report of the IFCN committee on basic mechanisms. *Electroencephalogr. Clin. Neurophysiol.*, 1990, 76: 481-509.

From EEG Source Localization to Source Imaging

M. Scherg

Department of Neuroscience, Albert Einstein College of Medicine, New York

In recent years, multiple source activities have been shown to underlie event-related potentials (ERP) as well as epileptiform EEG activity recorded from the human scalp. The increasing number of recording locations in EEG and MEG has made a separation of these source activities more and more feasible. In fact, the present advances in measurement and analysis techniques promise to lead to the development of a true "brain source imaging" in a double sense:

First, spatial images can be constructed from the measured scalp topographies using multiple source or minimum norm techniques. These images may be based on single time slices, on a specific frequency band or spatial patterns which integrate information over time or frequency, for example, by principal components or regional source analysis. In general, the spatial images are quite blurred, the more the lesser information is integrated over time or frequency. The spatial blurring is also dependent on whether or not the number of estimated parameters exceeds the number of measured variables. In this sense, minimum norm methods (underdetermined inverse problem) tend to result in increased blurring as compared to multiple source methods (overdetermined if appropriately defined as, e.g. in regional source imaging).

Second, the dynamic changes of the scalp EEG and ERPs over time require "brain source images" to comprise an image of the temporal evolution. The most simple answer to this would be a sequence of the blurred spatial images over subsequent time slices. We propose a physiologically more appropriate and better interpretable form of "brain source imaging", the imaging of source activity waveforms by optimized spatial operators. Each waveform should ideally depict the temporal evolution of the activity in a specific brain region. With this approach we shift our "focus of attention" away from "precise" localization to an optimal separation of the source activities from different brain regions. The goal of this approach is to "FOCUS" a "software lens" (Freeman 1980) onto different brain regions by optimizing the associated spatial operators for a specific electrode or sensor configuration, head model and data set. These operators can also be established without reference to a particular data set. However, this will decrease spatial resolution. The sensitivity of each spatial operator to source currents in different brain areas should be assessed in cross-sectional "sensitivity maps".

FURTHER READING

Scherg, M. Fundamentals of dipole source potential analysis. In: F. Grandori, M. Hoke and G.L. Romani (Eds.), Auditory evoked magnetic fields and electric potentials. *Adv.Audiol.*, Vol.6, Basel, Karger, 1990: 40-69.

Scherg, M. Functional imaging and localization of electromagnetic brain activity. *Brain Topography*, 1992, Vol.5, No. 2: 103-111.

Scherg, M. and von Cramon, D. Two bilateral sources of the late AEP as identified by a spatio-temporal dipole model. *Electroenceph. clin. Neurophysiol.*, 1985, 62: 32-44.

Scherg, M. and von Cramon, D. Evoked dipole source potentials of the human auditory cortex. *Electroenceph. clin. Neurophysiol.*, 1986, 65: 344-360.

Scherg, M. and Picton, T.W. Separation and identification of event-related potential components by brain electric source analysis. In: C.H.M. Bruna, G. Mulder, M.N. Verbaeten (Eds.), *Event-Related Potentials of the brain (EEG Suppl.42)*. Elsevier, Amsterdam, 1991: 24-37.

Scherg, M. and Ebersole, J.S. Models of Brain Sources. *Brain Topography*, 1993, Vol.5, No.4: 419-423.

Source Analysis of the Brain's Electromagnetic Signals

Matti Hämäläinen

Low Temperature Laboratory, Helsinki University of Technology
Espoo, Finland

The only two noninvasive methods which access the brain function with a millisecond time resolution are magnetoencephalography (MEG) and electroencephalography (EEG).

The neural activation is associated with an electric current, which is generally called the primary current, $\mathbf{J}^p(\mathbf{r})$. Both the magnetic field $\mathbf{B}(\mathbf{r})$, detected in MEG, and the electric potential $V(\mathbf{r})$, recorded in EEG, depend linearly on $\mathbf{J}^p(\mathbf{r})$. Given an electrode pair recording a voltage V_k and a MEG detection coil, recording a signal b_j , proportional to the magnetic flux threading the coil we can, therefore, write:

$$V_k = \int_G \mathbf{J}^p(\mathbf{r}) \cdot \mathbf{L}_k^E(\mathbf{r}) d\mathbf{v} \quad \text{and} \quad b_j = \int_G \mathbf{J}^p(\mathbf{r}) \cdot \mathbf{L}_j^M(\mathbf{r}) d\mathbf{v},$$

where the integration extends over the set G where $\mathbf{J}^p(\mathbf{r}) \neq 0$. The vector fields $\mathbf{L}_k^E(\mathbf{r})$ and $\mathbf{L}_j^M(\mathbf{r})$ are called the electric and magnetic lead fields, respectively. They depend on the sensor configuration and on the conductivity distribution within the head.

The analysis of the MEG and EEG signals involves the solution of the forward and inverse problems. The forward problem solution allows us to compute the lead fields to a good enough accuracy while the task in the inverse problem is to infer the primary current distribution on the basis of the measured signals and the known lead fields.

The MEG forward problem can be solved to good accuracy with relatively simple methods. If the head's conductivity distribution is assumed to be spherically symmetric, \mathbf{B} is given by a simple analytical formula, which does not depend on the radii of the different spherical layers or their conductivities. In contrast, the electric potential distribution is altered when the conductivities or layer thicknesses change. Since accurate conductivity data is not available this presents an important benefit for MEG.

If one wants to use a more sophisticated model with a realistic shape it is, again, simpler to compute \mathbf{B} than V . Because the conductivity of the skull is low, one can, to a good precision, use a single-compartment model where the skull and the scalp are replaced by a perfect insulator. The EEG computation, again, requires the knowledge of all conductivities with skull, scalp, and, possibly CSF taken into consideration.

Since the inverse problem does not possess a unique solution, additional information besides \mathbf{B} and V is required to set up a reasonable model for \mathbf{J}^p . A popular approximation is a set of current dipoles approximating small active regions in the brain. When the data can be explained by just one dipole, it is usually fairly simple to find the optimal solution. However, when one goes beyond this first-order model by assuming several dipole sources it is necessary to guide the fitting procedure manually by giving initial estimates. It is also helpful to consider a long time series together assuming that the same sources, with time-varying strengths, can account for the whole response.

In practice, it is beneficial if one can deduce an approximate solution directly from the raw data. Therefore, we have advocated the use of planar gradiometer sensors in MEG. They measure maximum signal just above the current source. We have found this feature very important in the analysis of the complex brain functions both in evoked response studies and in spontaneous activity recordings. The initial solution from the raw data can be refined in the actual model fitting procedure.

Higher Brain Functions Reflected in MEG

Mikko Sams

Low Temperature Laboratory, Helsinki University of Technology

The auditory cortex is very sensitive to changes in acoustical features of auditory stimuli. A deviant stimulus presented among identical standard stimuli elicits a mismatch response (MMR) in the auditory cortex. Any change, including frequency, spatial location and intensity, seems to elicit this robust response.

We recently showed that a change even in the direction of a frequency glide elicits an MMR. The deviants were identical to standards, but presented backwards. Because the long-term spectra of the 30-ms glides were identical, we argued that neurons tuned to frequency glides must be involved in the MMR generation. This interpretation is in line with psychoacoustical data demonstrating that detection of rising and falling glides can be independently adapted.

We also addressed whether the auditory cortex can differentiate the abstract feature of glide direction. In this study, the magnitude of the glides was one octave around the center frequency, which could obtain 16 different values ranging from 0.5 to 2.0 kHz. Again, the deviants and standards were otherwise identical, but of opposite direction. Amazingly, the deviants elicited an MMR, suggesting that auditory cortex can detect also abstract features of sounds.

In speech perception, one of key problems is how the perceptual system can deal with the immense amount of acoustical variation in normal speech. How does the perceiver detect the invariant features defining the phonemes. We attacked this problem by presenting to our subjects two synthetic syllables, /ba/ and /ga/. However, their fundamental frequencies were varied as if the same speaker had pronounced them at 16 different pitches. When presented as a deviant, the syllable elicited a strong MMR indicating that phonetically invariant information had been extracted at the level of auditory cortex from the extensive pitch variation.

In our recent study, we used as stimuli natural Finnish syllables /pa/ and /ka/. In the simple condition, the stimulus sequence consisted of these two syllables, spoken by one speaker. In a complex condition, the syllables were spoken by ten different speakers. The deviant syllable in the simple condition elicited a large MMR, as expected. However, this was not the case in the complex condition, even when there were two clear phoneme categories.

The above results suggest that auditory cortex is able to detect simple, complex and even abstract acoustical features of the sounds. This detection may occur in spite of variation on some other irrelevant stimulus feature. However, purely phonetic invariances are probably not found by the same mechanism.

Reactivity of Spontaneous MEG activity

Riitta Salmelin

Low Temperature Laboratory, Helsinki University of Technology
Espoo, Finland

Cortex supports joint oscillations of a large number of neurons, resulting in coherent rhythmic activity which can be measured on the surface of the cortex by electrocorticography (ECoG) and also from outside of the head, employing magnetoencephalography (MEG) and electroencephalography (EEG), which are completely non-invasive methods.

Cortical rhythms have been traditionally attributed to spontaneous activity in the occipital lobe and in the sensorimotor areas along central sulcus; temporal rhythmic activity has also been reported. In general, rhythms are suppressed in a cortical site when that area is exposed to stimulation or involved in a task. Suppression is occasionally followed by an enhancement, increasing above the base level amplitudes. Because of the performance-related suppression, the rhythms have been interpreted as an 'idling' state of the sensory cortices. They may also indicate that when performance level is low, the cortical areas increase their 'gain' to better resolve systematic features in the input, signalling relevant information. Typically, 10-Hz activity in the occipital lobe ('alpha') is suppressed when the subject opens the eyes or when he/she creates mental images of objects, eyes closed. Movement of body parts, most prominently that of fingers, suppresses the 10- and 20-Hz rhythms in sensorimotor cortex ('mu'), and a clear 'rebound' effect is often observed when the movement has ended.

It is likely that such coherent oscillations have a relevant role in brain function, despite the wide interindividual variability in abundance and intensity. The event-related changes of sensorimotor rhythms, in particular, have been studied in more detail. The temporal span of 10- and 20-Hz suppression clearly differs, implying that they are functionally distinct. However, the exact physiological significance of cortical rhythms still remains unclear.

Large cortical areas are generally involved in rhythmic activity, and the separate source sites are difficult to distinguish in EEG signals blurred by the presence of the skull and the scalp. ECoG provides accurate localization, but is only available from patients, typically suffering from epilepsy. To assign a definite function to a particular rhythm, we need to perform a multitude of repeated tasks, in healthy subjects and in normal conditions.

In this paper, we introduce combination of spectral information, event-related changes of frequency ranges during tasks, and the localization power of a whole-head neuromagnetometer to provide tools for characterization and quantification of cortical rhythms. Such methodology may assist us in an understanding of the physiological significance of rhythmic activity.

Half-Sensitivity Volumes in EEG and MEG Measurements

Veikko Suihko, Jaakko Malmivuo
Ragnar Granit Institute, Tampere University of Technology

1 INTRODUCTION

In 1819 Hans Christian Örsted demonstrated that when an electric current flows in a conductor, it generates a magnetic field around it. This fundamental connection between electricity and magnetism was expressed in exact form by James C. Maxwell in 1864. In bioelectromagnetism this means, that when electrically active tissue produces a bioelectric field, it simultaneously produces a biomagnetic field. Thus, the origin of both the bioelectric and the biomagnetic signals is the bioelectric activity of the tissue.

The electromagnetic connection in biological sources was first experimentally demonstrated by the first detection of the magnetocardiogram, MCG in 1963 by Baule and McFee. The first recording of the magnetoencephalogram, MEG, was made in 1968 by David Cohen. Since the first detection of the biomagnetic signals new diagnostic information or other clinical benefits from biomagnetic signals has been widely anticipated.

The biomagnetic detection of the bioelectric activity may introduce either technical or theoretical differences compared to the bioelectric method. The technical benefits include such as that the detection of biomagnetic signals may be done without fixing the electrodes on the skin. Also the superconducting SQUID detectors are capable of detecting DC-currents. On the other hand, the biomagnetic technology needs, especially in the brain studies, very expensive instrumentation and a magnetically shielded room.

The theoretical differences may be explained through the different sensitivity distributions of electric and magnetic measurement methods. In the sensitivity distribution we may discuss the form of the lead field and the detectors' ability to localize the source.

If the lead fields of two detection methods, independently whether these are electric or magnetic, are identical, the signals and thus their information contents are identical. In their basic form the electric and magnetic lead fields are independent. Thus they detect different aspects of the source and contain different information, though not being fully independent (Malmivuo and Plonsey, 1994).

When considering the detector's ability to localize the source we may define a new concept called half-sensitivity volume. This concept means the volume, where the detector's sensitivity is more than one half of its maximum value in the source region. The smaller the half-sensitivity volume, the smaller the region from where detector's signal originates is.

In this paper we review the form of EEG and MEG lead fields which are already published elsewhere (Malmivuo, 1980; Malmivuo, 1993; Malmivuo and Plonsey, 1994; Malmivuo and Suihko, 1993) and describe the behavior of the half-sensitivity volumes as a function of detector distance.

2 MODELS AND METHOD

2.1 Head models

For calculating the lead fields and half-sensitivity volumes two models are used. The lead fields for the EEG-electrodes and axial magnetometer are calculated in the spherical head model introduced by Rush and Driscoll (Rush and Driscoll, 1969). For the planar gradiometer the half-space model is used.

The spherical model is selected because of its mathematical simplicity and because in a limited region close to the detector it may be considered very accurate. Thus it can be considered to represent the volume conductor of the head accurately enough. In calculating the lead fields for the axial gradiometer, due to cylindrical symmetry, the results in the brain region are not affected by the inhomogeneities of the model. In the application of the planar gradiometer the half-space model is used in the calculations because the spherical model does not exhibit cylindrical symmetry for coplanar gradiometer coils. If the planar gradiometer coils are not coplanar but coaxial with the head model, the spherical model can be easily applied. With short baselines the half-space model gives results which are applicable with reasonable accuracy to the real head.

2.2 Electric leads

The electric leads include two and three electrodes. The dimension of the electrodes is considered infinitesimally small. In the two-electrode lead the distance between the electrodes varies between 0 and 180 degrees. In the three electrode lead the third electrode is added in the middle of the aforementioned two electrodes so that the middle electrode forms one terminal and the lateral electrodes are connected together to form the other terminal.

A special case of the electric leads is that where the lead field of only one electrode is considered. This unipolar lead may be that of either the two- or the three-electrode lead.

The equations for calculating the electric lead fields and half-sensitivity volumes are not given here. They can be found from (Rush and Driscoll, 1969; Puikkonen and Malmivuo, 1987; Suihko and Malmivuo, 1993).

2.3 Magnetic leads

Coil size and measurement distance

Two kinds of magnetometer configurations are used. These are axial and planar gradiometers. In both cases the magnetometer coils have the radius of 10 mm. The distance of the detector coil from the scalp is 20 mm being thus 32 mm from the surface of the brain. This is practically the minimum recording distance for a superconducting magnetometer coil. It has been shown by Malmivuo and Plonsey (Malmivuo, Plonsey, 1994) that even at this minimum distance decreasing the magnetometer coil radius does not change the form of the lead field. Therefore, the results obtained in this paper are also applicable for any coils with smaller than 10 mm radius.

Axial gradiometer

For the axial gradiometer the calculations are made as a function of the baseline. In MEG measurements the baselines usually vary between 30 and 100 mm. When the baseline is infinite the gradiometer can be considered as a single-coil magnetometer.

Planar gradiometer

Also for the planar gradiometer the calculations are made as a function of the baseline. The coils are considered coplanar and the model is half-space model. This model is relevant because the calculations are made only for a limited range of the baseline. With this range of the baseline the results would be practically the same if the coil were coaxial with the spherical head model. Note, that in that case the 180° separation would correspond to the arrangement of two magnetometers at opposite sides of the volume conductor.

The equations for calculating the magnetic lead fields and half-sensitivity volumes are not given here. They can be found from (Malmivuo, 1976; Malmivuo, 1993; Malmivuo and Plonsey, 1994).

2.4 Lead field

The sensitivity distributions are calculated by using the lead fields. The lead field is the electric current field in the volume conductor raised by feeding a unit current to the lead. Due to the reciprocity theorem of Helmholtz the lead field is the same as the distribution of the sensitivity of the lead.

Display of results

The lead fields are displayed with lead field current flow lines (thin solid lines). The illustrations also include the isosensitivity lines (dashed lines). The half-sensitivity volumes are indicated with shading. For the planar gradiometer the lead field is displayed also with lead field current density vectors in a rectangular grid.

The half-sensitivity volumes are displayed as a function of detector distance. This is given both in degrees and in circumferential distance. For the planar gradiometers the circumferential distance means, of course, the distance of the projections of the coil centers on the scalp. For axial gradiometers the magnetometer baseline is given on the same distance scale though as concept it is not directly commensurable with the planar gradiometer baseline distance. The half-sensitivity volumes are given in cubic centimeters of brain region volume. Another scale gives this in percentage from the volume of the sphere representing the brain region. Note, that in reality the brain fills perhaps only one half of this sphere.

The general sensitivity of the lead is also an important factor for practical measurements. Therefore, the maximum sensitivities of EEG and MEG leads are presented as a function of the detector separation.

3 RESULTS

3.1 Form of the lead fields

Electric leads

Examples of the form of the lead fields for the two and three-electrode leads are shown in Figure 1. Due to the insulating effect of the skull the sensitivity is quite homogeneously distributed within the brain region. At large electrode distances it is directed mainly radially. At small electrode distances it is directed mainly tangentially. With the three-electrode arrangement the sensitivity is directed always mainly radially, although with small electrode distances also some tangentially directed sensitivity is present. Note, that when the separation of the distal electrodes in the three-electrode lead reaches 360° it is identical to the two-electrode lead with 180° electrode separation.

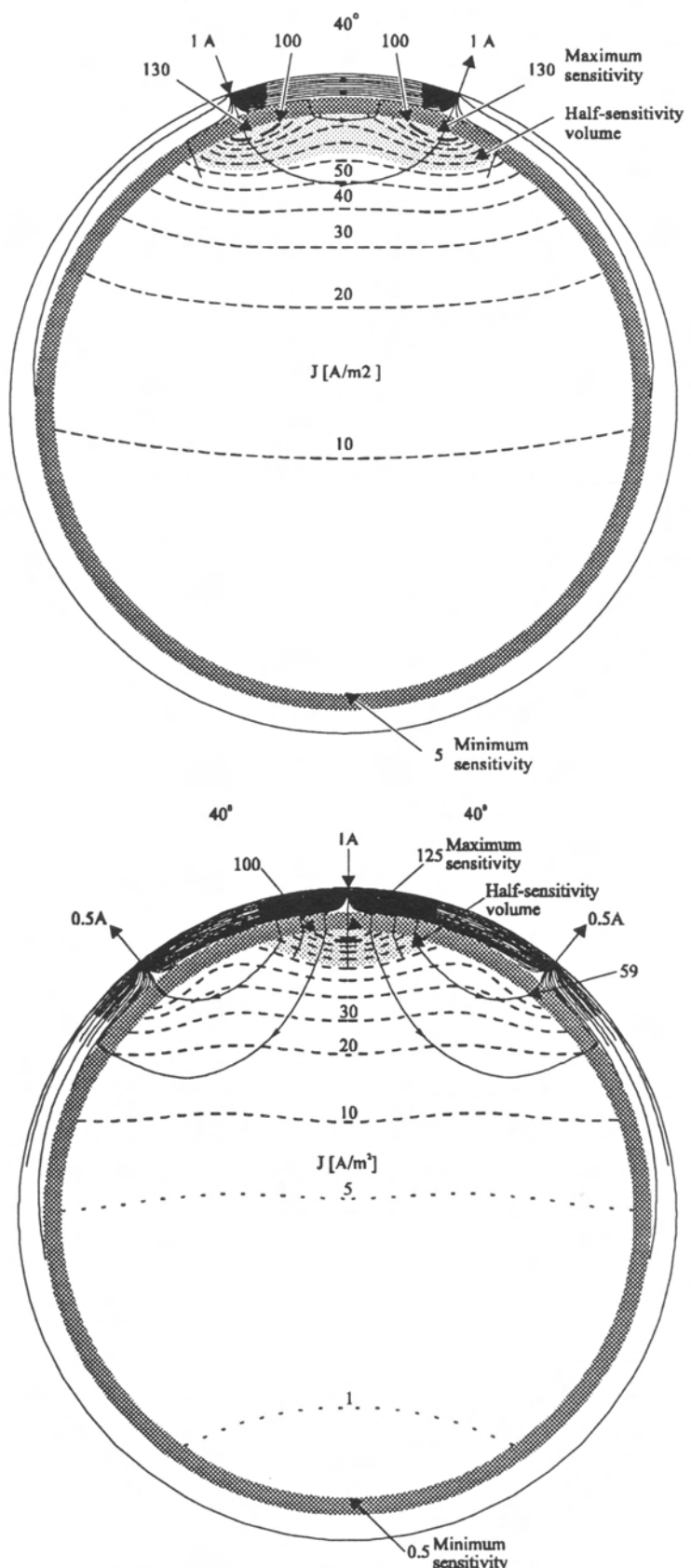


Figure 1. The lead fields for two-electrode and three-electrode electric leads with the electrode separation of 40°. Thin solid lines are lead field current flow lines and dashed lines are isosensitivity lines. The half-sensitivity volumes are indicated with shading.

Magnetic leads

The form of the lead field for a magnetometer, which is same as an axial gradiometer with infinite baseline, is shown in figure 2. The axial gradiometer has a tangential sensitivity distribution throughout the brain region independently of the baseline. The sensitivity is tangential not only to the surface of the brain but to the symmetry axis of the magnetometer. Therefore, we call its form vortex. The sensitivity is zero at the symmetry axis and increases as a function of the radial distance from the symmetry axis.

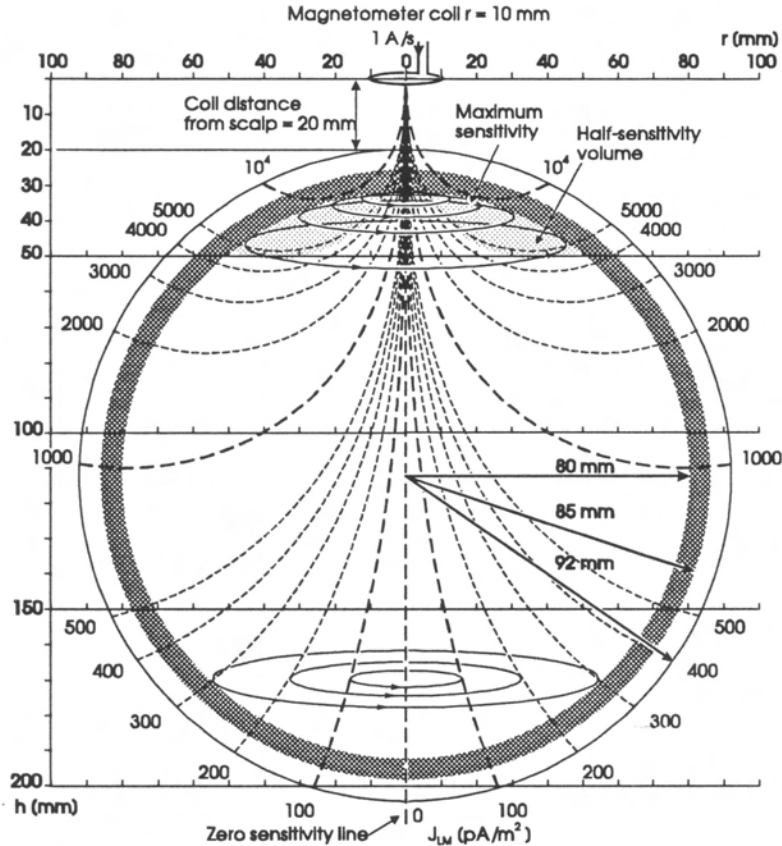


Figure 2. The lead field for magnetometer, also for axial gradiometer with infinite baseline. Thin solid lines are lead field current flow lines and dashed lines are isosensitivity lines. The half-sensitivity volumes are indicated with shading.

The lead field for a planar gradiometer is presented in figures 4 and 5. The planar gradiometer has also a tangential sensitivity distribution. Because at small baselines the coil configuration is quadrupolar, the sensitivity has its maximum value under the common center of the two coils. The sensitivity is linearly directed. At large baselines close to 180° the sensitivity is similar to that of axial gradiometers.

3.2 Half-sensitivity volumes

Electric leads

Half-sensitivity volumes are presented in figure 5 as a function of detector separation. With the two-electrode lead the minimum of the half-sensitivity volume is obtained at separation of 5° or less. Then it increases as a function of distance having its maximum at about 60° separation. Between 60° and 180° separations the half-sensitivity volume is relatively independent of the electrode distance.

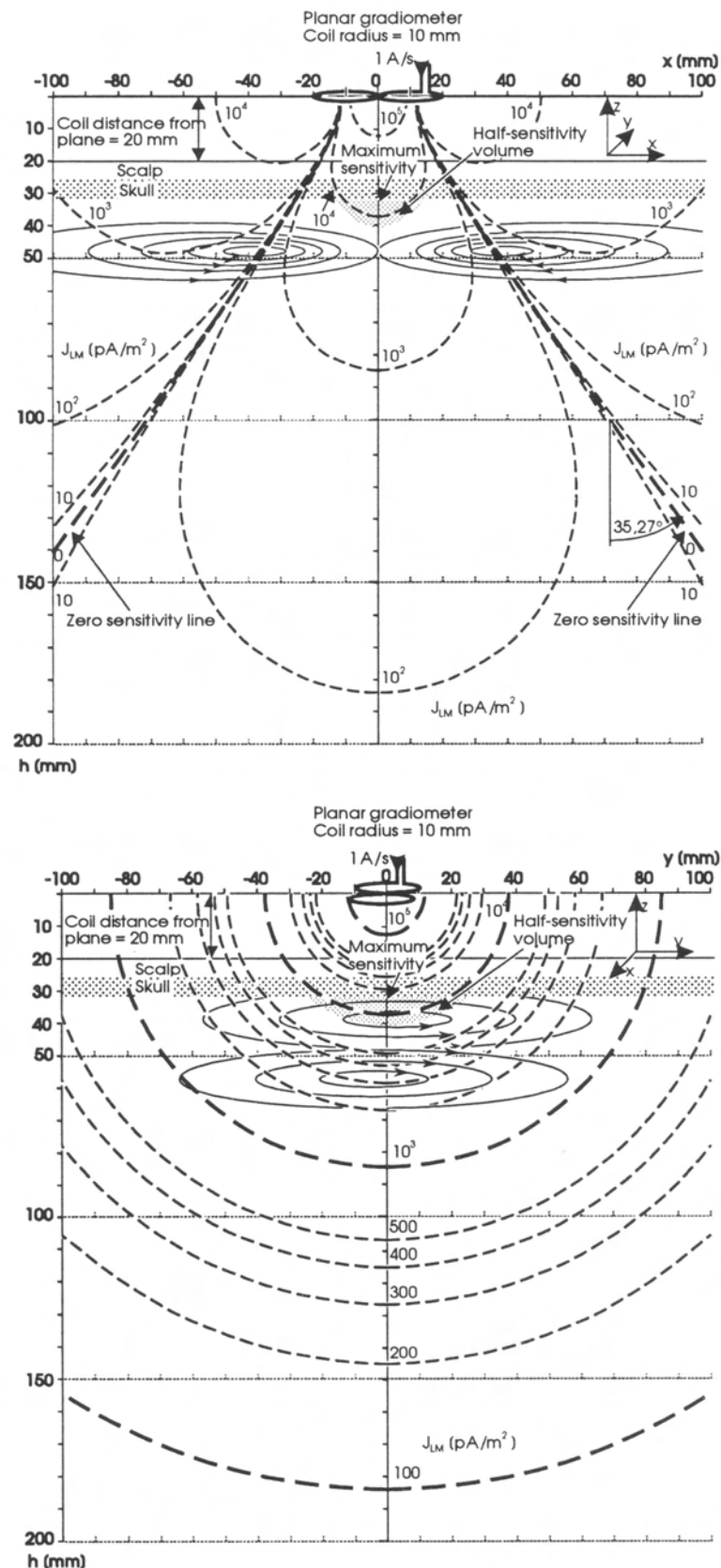


Figure 3. The lead field for planar gradiometer viewed from two directions. Thin solid lines are lead field current flow lines and dashed lines are isosensitivity lines. The half-sensitivity volumes are indicated with shading.

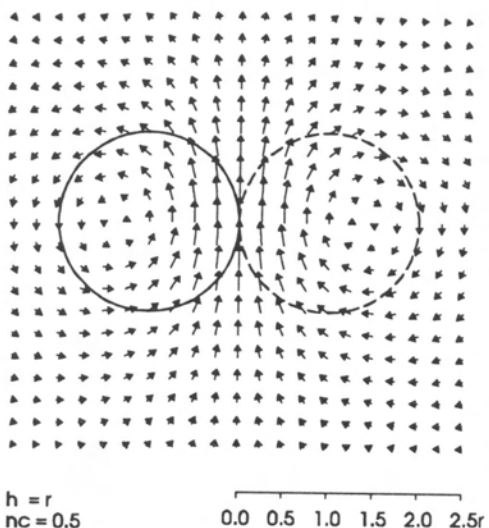


Figure 4. The lead field for planar gradiometer presented as matrix of lead field current density vectors. The field is viewed from above (see figure 3) and the distance from the gradiometer is same as the radius of the coils.

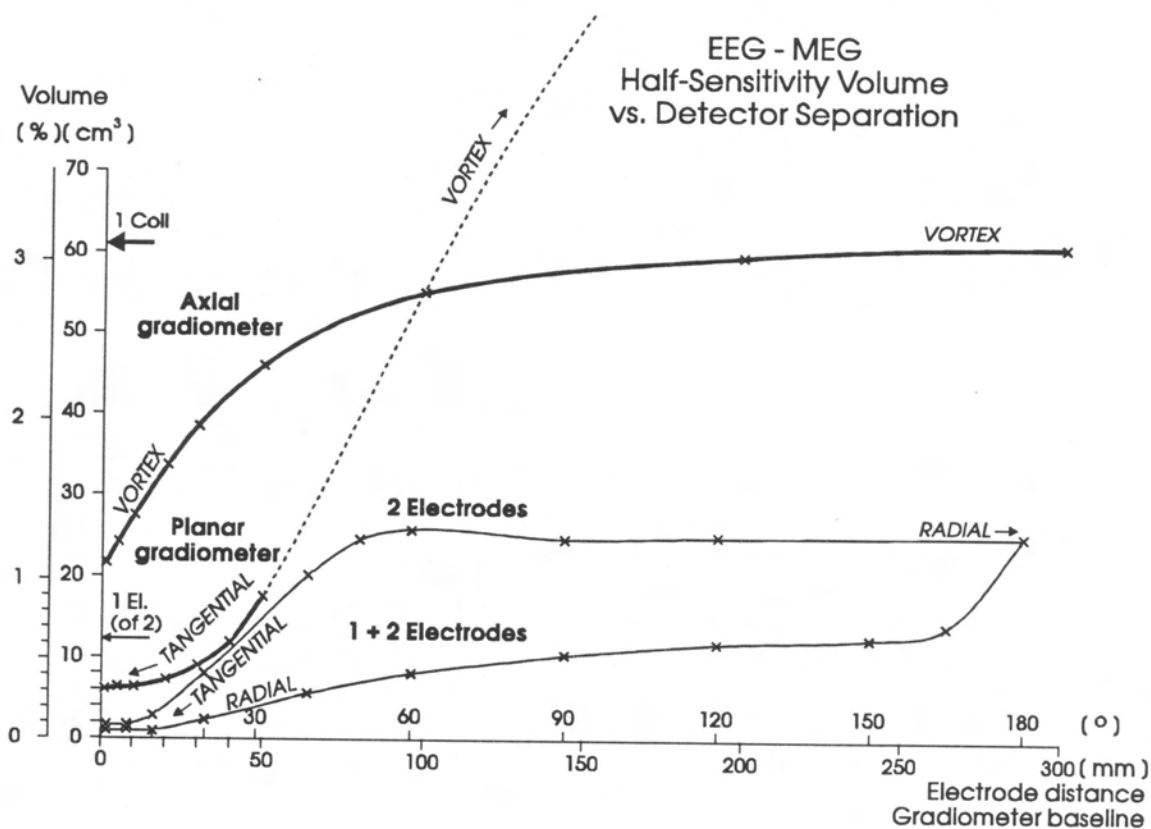


Figure 5. The half-sensitivity volume as a function of the detector separation for axial and planar gradiometers and two- and three-electrode electrical leads. The detector separation is given both in degrees and circumferential distance. The half-sensitivity volume is given in cubic centimeters and alternatively in percentage from the volume of the sphere representing the brain .

At small baselines the half-sensitivity volume of the three-electrode lead is about 30% of that of the two-electrode lead. The half-sensitivity volume increases monotonically as a function of electrode separation. When the distal electrode separation reaches 360 mm the half-sensitivity volume is equal to that of the two-electrode arrangement.

Magnetic leads

The half-sensitivity volume of axial gradiometer is smallest with small baselines and increases as a function of baseline approaching that of a single coil magnetometer. At small baselines the half-sensitivity volume of the planar gradiometer is significantly smaller than that of the axial gradiometer. At very large separation the half sensitivity volume of planar gradiometer is about twice that of the axial gradiometer.

3.3 Maximum sensitivities

Maximum sensitivities as a function of detector separation are presented for EEG leads in figure 6 and for MEG leads in figure 7. As compared with changes in the half-sensitivity volumes the changes in the sensitivities are well acceptable. For example if the electrode distance of the two-electrode lead is halved from 50 to 25mm the maximum sensitivity is still about 80% of the one with 50mm, where as the half-sensitivity volume is decreased very significantly.

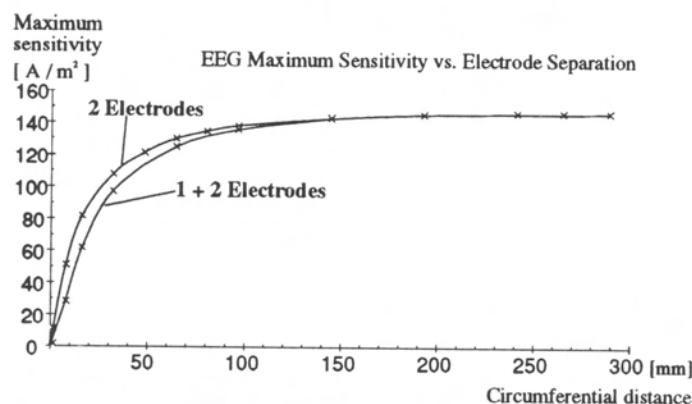


Figure 6. Maximum sensitivity as a function of electrode circumferential distance for two-electrode and three-electrode electrical leads.

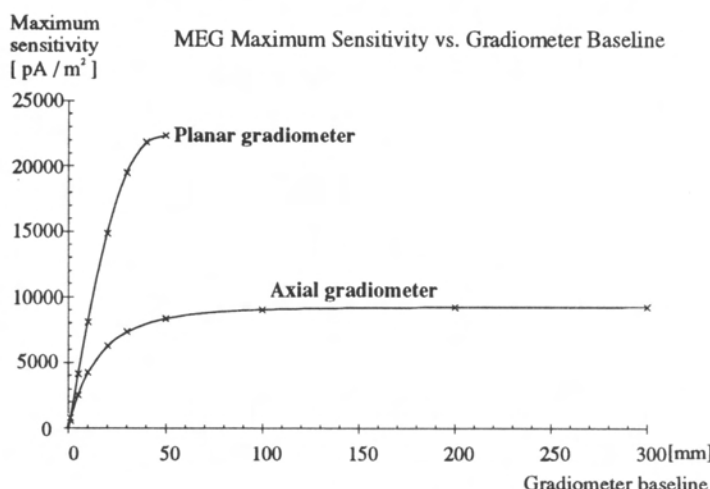


Figure 7. The maximum sensitivity as a function of baseline for axial and planar gradiometer.

4 DISCUSSION

4.1 Form of the lead fields

The radially oriented lead field of a single electrode cannot be synthesized with any magnetic lead. Similarly the vortex field of an axial magnetometer cannot be synthesized with any electric lead. Thus it may be assumed, that these leads give most complementary information about the electric sources of the brain.

With short baselines the lead fields of the two-electrode lead and the planar gradiometer resemble very much each other. Thus the information from these leads may be expected to be most redundant between electric and magnetic leads.

4.2 Size of the half sensitivity volume

Despite of the diffusing effect of the skull the electric leads seem to have very small half-sensitivity volumes if the electrode separation is small. Especially the three-electrode lead is superior as compared with other leads. Also the planar gradiometer has a small half-sensitivity volume with a small baseline. The half-sensitivity volumes obtainable with the axial gradiometer are quite large.

4.3 Effect of the head model

The effect of the high resistivity skull to the electric lead fields is so dominating that the results of this paper should be carefully examined with different skull resistivities and anatomical measures. As for the magnetic lead fields with the axial gradiometer deviation from the cylindrical symmetry of the brain-skull boundary may have some effect.

5 SUMMARY

Considerable scientific and economic investments are made in biomagnetic brain research. The biomagnetic instrumentation is at least 25 times more expensive than a corresponding bioelectric instrumentation (Wikwo, Gevins, and Williamson, 1993). However, both bioelectric and biomagnetic methods detect the same fundamental physiological phenomenon, i.e. the electric activity of the brain.

The bioelectric and biomagnetic method have both technical and theoretical differences. In this paper we have discussed their theoretical differences by examining their lead fields. In this discussion we have considered both the forms of the lead fields and the sizes of the half-sensitivity volumes for one-, two-, and three-electrode electric leads and for axial and planar gradiometers.

The analysis has shown that the one-electrode electric lead and axial gradiometer magnetic lead have independent lead fields and thus the information content obtained with these leads may be expected to be most independent.

The form of two-electrode electric lead and planar gradiometer magnetic lead resemble each other so much that it may be expected that the information content of these leads is most redundant.

In summary, at very small separations the half-sensitivity volume of planar gradiometer is less than one third of that of axial gradiometer, and that of two-electrode lead is further less than one third of that of planar gradiometer. The three-electrode lead has the smallest half-sensitivity volume.

To assess the clinical diagnostic value of magnetoencephalography and to be able to justify its much higher price compared to a comparable electric method, the bio-

magnetic studies should be done parallel with comparable bioelectric studies. In this way it is possible to evaluate the independence of the information obtained with these two methods.

6 REFERENCES

- Malmivuo JA (1976): On the detection of the magnetic heart vector - An application of the reciprocity theorem. *Helsinki Univ. Tech.*, Acta Polytechn. Scand., El. Eng. Series. Vol. 39., pp. 112. (Dr. tech. thesis)
- Malmivuo JA (1980): Distribution of MEG detector sensitivity: An application of reciprocity. *Med. & Biol. Eng. & Comput.* 18:(3) 365-70.
- Malmivuo, (1993); Sensitivity distribution of MEG measurement and energy distribution in magnetic stimulation of central nervous system. *Abstracts of 2nd Far Eastern Conf. on Med. Biol. Eng.*, Aug 15-18 1993, Beijing China, p. 370.
- Malmivuo JA and Plonsey R (1994): *Bioelectromagnetism - Principles and Applications of Bioelectric and Biomagnetic Fields*. Oxford University Press, in press.
- Malmivuo JA, Puikkonen J (1987): Sensitivity distribution of multichannel MEG detectors. In *Abst. 6th Internat. Conf. Biomagnetism, Tokyo, 27-30 August*, ed. K Atsumi, M Kotani, S Ueno, T Katila, SJ Williamson, pp. 112-3, Tokyo Denki University Press, Tokyo.
- Malmivuo JA, Puikkonen J (1988): Qualitative properties of the sensitivity distribution of planar gradiometers. *Tampere Univ. Techn., Inst. Biomed. Eng., Reports* 2:(1) pp. 35.
- Puikkonen J, Malmivuo JA (1987): Theoretical investigation of the sensitivity distribution of point EEG-electrodes on the three concentric spheres model of a human head - An application of the reciprocity theorem. *Tampere Univ. Techn., Inst. Biomed. Eng., Reports* 1:(5) 71.
- Rush S, Driscoll DA (1969): EEG-electrode sensitivity - An application of reciprocity. *IEEE Trans. Biomed. Eng.* BME-16:(1) 15-22.
- Suihko V, Malmivuo JA, Eskola H (1993): Distribution of sensitivity of electric leads in an inhomogeneous spherical head model. *Tampere Univ. Techn., Ragnar Granit Inst., Rep.* 7:(2) .
- Wikswo JP, Gevins A and Williamson SJ (1993): The future of the EEG and MEG. *EEG clin. Neurophys.* 87: 1-9.

EEG and MEG Signal Analysis

The Integration of EEG, MEG and Magnetic Resonance Imaging

S.R.Walker¹, C.N. Guy² and S.J.M Smith³.

¹ Ragnar Granit Institute, Tampere University of Technology, SF 33101 Tampere, Finland.

² Physics Department, Imperial College of Science, Technology & Medicine, London SW7 2BZ.

³ Department of Clinical Neurophysiology, National Hospital for Neurology & Neurosurgery, London, WC1E.

Abstract

This paper describes the basic concepts of a combined EEG/MEG/MR imaging system designed to localise the cortical generators of scalp EEG and surface MEG fields. The guiding philosophy of this work is to unite structural information about the brain provided by high-resolution magnetic resonance images with the functional information from EEG and MEG.

It is anticipated that this combined approach will produce physiologically reasonable solutions describing the location and propagation of electrical activity at the cortical level.

Background: A Comparative Study of EEG and MEG in Epilepsy

The relationship between MEG and EEG in epilepsy has been studied at Imperial College over the past five years. Three patient groups were studied. The first comprised patients with intractable temporal lobe epilepsy undergoing assessment for neurosurgery at the Maudsley Hospital, Denmark Hill, London. The majority of these patients were believed to have hippocampal foci of idiopathic origin. The second group comprised patients with well controlled idiopathic epilepsies of cortical origin, with foci in the temporal or parietal lobes. These patients were referred by the National Hospital for Neurology and Neurosurgery, Queen Square, London. The third group comprised epileptic patients with a variety of cortical malformations, some associated with neuronal migration defects. Again, these patients were referred by the National Hospital for Neurology.

The surgical patients underwent simultaneous interictal scalp EEG, foramen ovale (F.O.) subdural EEG and MEG recording. Access was also provided to the patients' previous EEG histories comprising a large number of standard scalp EEG records, recordings with scalp EEG and up to 12 channels of subdural (F.O.) EEG and depth records with as many as 32 channels. This material included ictal as well as interictal recording.

The National Hospital patients also underwent simultaneous EEG and MEG recording and access was also provided to their EEG histories.

Two MEG instruments were used. Both instruments were designed and built at Imperial College. The first system was a single-channel D.C. SQUID magnetometer with second order axial gradiometer (diameter 35mm, baseline 46mm) operating with a noise figure of approximately 10fT/ $\sqrt{\text{Hz}}$ in an unscreened laboratory. The second system was a 7-channel R.F. SQUID magnetometer with identical second order

gradiometers operating with a noise figure of $22-24\text{fT}/\sqrt{\text{Hz}}$ in the same unshielded environment.

Analysis of simultaneous scalp EEG, Foramen Ovale EEG and MEG from the group of surgical patients revealed important differences in the epileptic activity recorded by EEG and MEG. The following points summarise the findings:

1. MEG wave morphologies often differed greatly from those exhibited by the scalp and subdural EEG.
2. With the magnetometer in an unchanged position, consecutive epileptic events which produced almost identical EEG field distributions, generated markedly different MEG signals.
3. Timing differences (10 - 40ms) were often apparent between the onset of epileptic activity in the EEG and MEG records. These could not be accounted for by inter-channel differences in filter parameters.

Comparison of the MEG and scalp EEG records from the two other patient groups confirmed these findings. Examination of the multi-channel depth recordings from the surgical patient group revealed similar waveform and latency differences within the electric record.

Observations (1), (2) and (3) suggested the following conclusions:

1. The waveform differences between the EEG and MEG records suggested that the two techniques were sensitive to different components of the underlying activity.
2. The delay between the onset of activity in the EEG and MEG records and those observed within the electrical record suggested that epileptic events were actively propagated within the brain.
3. The changes in MEG wave morphology between consecutive events producing similar EEG fields suggested that MEG was the more sensitive indicator of changes in source configuration due to propagation of epileptic activity across the cortex.

In an attempt to verify these conclusions, a simple computer brain model was constructed. This comprised a realistically shaped two-dimensional cortical section. The outline was assumed to exist within a homogeneous spherical volume conductor. Starting from any point on the outline, the cortical surface could be populated with current dipole sources. The sources were equally spaced and oriented normal to the local surface vector. The extent of the source could be varied by changing the number of dipoles. The potential field and normal component of the magnetic field were calculated at the surface of the spherical volume conductor, assuming all dipoles were activated simultaneously and in the same sense.

It was found that varying the location and/or extent of the source simulated the relationship between MEG and EEG fields observed experimentally. Specifically, it was possible to reverse the sense of the magnetic field while maintaining almost identical electric field distributions, a phenomenon which had been observed on a number of occasions in real recordings.

Figure 1 illustrates a possible explanation of this effect. Here a source comprising a fixed number of dipolar elements, always oriented perpendicular to the local cortical surface, propagates across the cortex, traversing a sulcus. In the spherical homogeneous conductor model, contributions to the radial component of the magnetic field arise only from current sources tangential to the surface of the sphere. Thus, the majority off the magnetic signal arises from current sources in the walls of the sulcus. The surface potential field, on the other hand, contains contributions from both radial and tangential current sources. As the extended source propagates from one side of the sulcus to another, the magnetic field undergoes a polarity reversal, passing through zero when both walls of the sulcus are equally populated. Model calculations of the potential and magnetic field distribution during this process reveal that reversal of the magnetic field is accompanied by much less significant changes in the electric potential distribution.

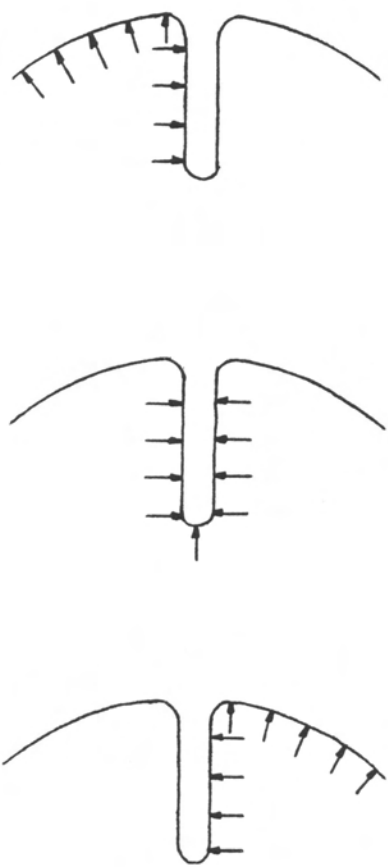


Figure 1 Propagation of an Extended, Multi-Dipolar Source Across a Sulcus

Motivation for Three-Dimensional Source Modelling Using Magnetic Resonance Images

Source modelling in EEG and MEG research often involves the localisation of equivalent current dipole sources. The dipole coordinates, orientations and moments are often calculated iteratively. An initial source position and orientation are chosen, the magnetic or potential field due to the current dipole is calculated and compared

with measured fields. The dipole parameters are adjusted until a best-fit to the measured fields is obtained. The brain is often modelled as a homogeneously conducting sphere. The final solution for dipole coordinates and orientation is generally unconstrained: the source is permitted anywhere inside the spherical volume conductor and the dipole may assume any orientation.

As magnetic resonance imaging has become more widely used, MR images have been incorporated into MEG and EEG source localisations. Typically, the images are used to construct best-fitting spheres which model the brain, skull and scalp. Calculation of dipole parameters proceeds as before and the final results are superimposed on the MR images so that the source localisation may be correlated with anatomical features.

Application of the equivalent current dipole and spherical volume conductor model presents a number of difficulties. A key issue is the true nature of current sources within the brain. A best-fitting current dipole is by definition a hypothetical point source which could give rise to the observed fields. It is not the only possible solution and need have no physiological significance. For this reason, and because the dipole coordinates may assume any value within the volume conductor, source localisations involving single equivalent current dipoles often produce physiologically unreasonable results. A source may be predicted in a region where there is no active neuronal tissue, in the ventricles or white matter, for example.

The comparative study of EEG and MEG in epilepsy conducted at Imperial College and similar work elsewhere suggests that real EEG/MEG sources are extended and possess dynamic properties. There is also evidence for neuronal propagation of activity. This further challenges the equivalent current dipole and homogeneously conducting sphere model, where the volume conductor is assumed to be a passively conducting ohmic medium.

A Possible New Approach to Closer Integration of EEG, MEG and MRI

The uncertainties surrounding the nature of cerebral current sources and the apparent success of the two-dimensional extended cortical source model have led to the development of a combined EEG, MEG and MR imaging system at Imperial College.

The system was designed with the following aims:

1. to produce physiologically reasonable source localisations which explain epileptic seizure activity, using extended current sources confined to the surface of the cortex;
2. to investigate the relationship between EEG and MEG fields, providing greater insight into the true nature of electrical activity within the brain;
3. to integrate functional information from EEG and MEG more fully with structural information provided by magnetic resonance images.

The imaging system is a three-dimensional generalisation of the extended current source model described earlier. Instead of using a simplified cortical outline, a set of MR images comprising 124 coronal sections 1.5mm thick is used to define the precise outline of the cortex. Regions of the cortical surface are then populated with

multiple current dipole sources to form an extended, sheet-like source, following the convolutions of the cortex. As in the two-dimensional example, all dipolar source elements are oriented normal to the local surface vector. Surface EEG and MEG are calculated using a three-sphere conductor model. The radii of the spheres are determined with reference to the MR images.

The system is based on an IBM PC 486 computer (50MHz or higher). In addition to the features specific to EEG/MEG source localisation, it incorporates the following standard image processing functions:

1. display of magnetic resonance images in coronal, transaxial and sagittal format;
2. reformatting of MR images (i.e. construction of transaxial images from a set of coronal slices);
3. image enhancement using anti-aliasing techniques, contrast adjustment and thresholding;
4. three-dimensional reconstruction of the whole head, cortical surface or grey-white matter boundary.

It should be noted that this approach has a number of novel features:

1. Structural information from the MR images is used to constrain the possible source locations to regions which contain active neuronal elements. Sources are not permitted in physiologically unreasonable locations.
2. Because the sources are confined to the cortical surface the model is patient-specific and unique.
3. Other imaging techniques may also be incorporated. For example PET images showing increased/decreased metabolism in certain regions of the brain could be used as a guide to source location and extent.

Correlated Noise Sources of EEG in Anaesthesia: an Application of Average Mutual Information Based Multivariate Autoregressive Model

Pekka Loula, Kari Mäkelä*, Ville Jäntti*, Jaakko Astola**

Technical Research Centre of Finland, Medical Engineering Laboratory
P.O.Box 316, FIN-33101, Tampere, Finland
Fax: +358 31 174 102, e-mail: loula@sai.vtt.fi

*Tampere University Hospital, Clinical Neurophysiology

**Tampere University of Technology, Signal Processing Laboratory

Through last decades physiological systems have been modelled intensively with linear methods. Although efficient methods for nonlinear modelling have been introduced, e.g. Wiener modelling, nonlinear neural networks, deterministic chaos modelling, nonlinear autoregressive models (state space modelling, bilinear models), etc., their use have been limited in modelling physiological systems. All biological systems, however, including cardiovascular-, respiratory-, and central nervous systems, contain nonlinearities which can not totally modelled with traditional linear methods.

Electroencephalogram (EEG) reflects the integrated electrical activity of a large number of neurons. The nervous system is affected more profoundly by anaesthetics than other systems of the body. At a low concentrations most anaesthetics show similar EEG patterns, but at higher concentrations specific patterns for different agents appear. The objectives to use EEG monitoring during surgery are prevention of brain damage, detection of EEG abnormalities at the time of their occurrence and prediction of post-operative neurologic outcome. The physiological state of the patient, such as hypothermia, hypotension and hypoxia, other used drugs and physiological interventions during anaesthesia have also their own effects on EEG.

In this paper we introduce a method to model multi-channel EEG-recordings using closed-loop multivariate autoregressive regressive (MAR) modelling. The closed-loop MAR-model explains all the observed measurements by a sum of its own noise source and correlated noises sources with other measurements. Typically in analyzing EEG-measurements with MAR-model there is very strong correlation between different derivations preventing further usage of the model e.g. in describing transfer functions between measurements. We are interested in studying correlated noise sources it selves and to compare the results obtained with linear and nonlinear MAR-model, i.e. determined using auto- and cross correlation functions and average mutual information (AMI) respectively.

Analysing EEG with average mutual information based MAR-model

A multivariate autoregressive (MAR) model identifies linear dependencies between several univariate random processes $x_i(k)$, $i = 1, 2, \dots, m$ related to each other. In MAR-modelling the value of a time series, i.e. measured signals, is described as a linear

combination of its past values $x_i(k)$ and an additive error term $e(k) = [e_1(k), e_2(k), \dots, e_m(k)]^T$ presenting the one-step prediction error. In other words, it is a linear model of the studied signal where all measured signals are outputs of studied processes describing each other and inputs are noise sources independent from each other, which imports to the system power. Using these features the analysis of the dynamics of the system can be performed with the MAR-model.

$$x(k) = \sum_{i=1}^M a(i)x(k-i) + e(k), \quad (1)$$

$$\text{where } a(i) = \begin{pmatrix} a_{11}(i) & a_{12}(i) & \dots & a_{1m}(i) \\ a_{21}(i) & a_{22}(i) & \dots & a_{2m}(i) \\ \vdots & \vdots & & \vdots \\ a_{m1}(i) & a_{m2}(i) & \dots & a_{mm}(i) \end{pmatrix}, i = 1, 2, \dots, M \quad (2)$$

where the error term $e(k)$ is a stationary zero mean white process, $x(k)$ is a multivariate stochastic process, $a(i)$ is a coefficient matrix with a time instant i , M is the number of output signals in model and m is model-order indicating how many previous samples are taken into account determining new $x(k)$ values. Signal $x(k)$ can be presented as an output on multivariate filter, the input of which $e(k)$ and correlation function can be estimated [Priestley, 1981] according to

$$E\{e(i+k)e(i)^T\} = \delta(k)\Sigma \quad (3)$$

$$\text{where } \Sigma = \begin{pmatrix} \sigma_{11}(i) & \sigma_{12}(i) & \dots & \sigma_{1m}(i) \\ \sigma_{21}(i) & \sigma_{22}(i) & \dots & \sigma_{2m}(i) \\ \vdots & \vdots & & \vdots \\ \sigma_{m1}(i) & \sigma_{m2}(i) & \dots & \sigma_{mm}(i) \end{pmatrix}, i = 1, 2, \dots, M \quad (4)$$

$$\text{and } \delta(k) = \begin{cases} 1, & k = 0 \\ 0, & k \neq 0 \end{cases} \quad (5)$$

where Σ is variance-covariance matrix of noise sources, diagonal element σ_{ii} of Σ describe variance of noise source and non-diagonal element σ_{ij} of Σ describe covariance of two noise sources e_i and e_j . Assuming that the MAR-model contains all internal dependencies of the multivariate system, then variance-covariance matrix with non-diagonal elements near zero manifests the absence of correlated noise sources and, on the contrary, values of non-diagonal elements near one reveal a strong correlated noise source between two channels.

In Figure 1 is depicted the generalized linear model of a dynamic closed-loop system with seven variables and one common correlated noise source n_e . The closed-loop model assumes that there are not any significant noise sources, which imports power to the system, except those included in the MAR-model. If there are not any significant correlated noise sources the model has a close correspondence to the real investigated phenomena and it can be used in predicting coming samples, investigating transfer functions etc..

Average mutual information (AMI) was presented in 1948 by Shannon [Shannon, 1948; Shannon 1949] and deepened by Gel'fand and Yaglom [Gel'fand and Yaglom, 1959] as a measure for the amount of information contained in a message in the area of communication systems. The general equation for continuous average mutual information $I(S, Q)$ is determined as

$$I(S, Q) = \int P_{sq}(s, q) \log_2 \left[\frac{P_{sq}(s, q)}{P_s(s)P_q(q)} \right] ds dq \quad (6)$$

where P_{sq} is the joint probability distribution function, P_s is the probability distribution function of S and P_q is the probability distribution function of Q . The average mutual information is a generalization of linear correlation function to the non-linear world, because it is defined by the joint probability distribution function P_{sq} and not by the variables s and q . When the measurement of system Q and system P are independent from each other, the $P_{sq}(s, q) = P_s(s)P_q(q)$ causing $I(S, Q)$ to be zero. The required joint probability distribution function can be estimated from histograms using e.g. method described by Fraser [Fraser 1986].

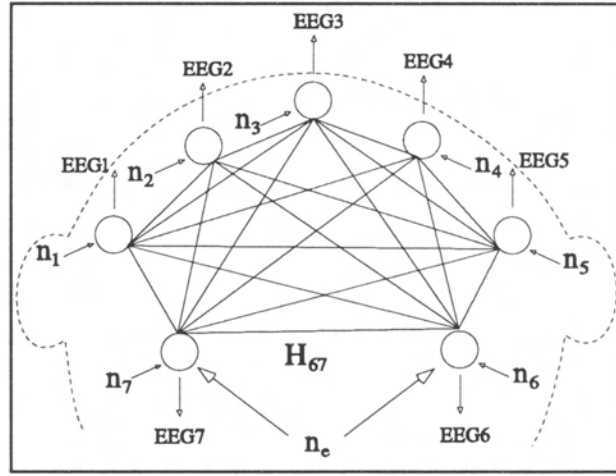


Figure 1. The effect of correlate noise source n_e in general closed-loop MAR model with seven variables. Each output signal is described by impulse responses from every other node and its own noise source.

A very interesting question in our case is: what happens in MAR-model and especially in the variance-covariance matrix if the multivariate correlation matrix $a(i)$ is determined on the basis of multivariate average mutual information matrix?. This makes it possible to take into consideration better the non-linear features of studied processes in the brain. Average mutual information is scaled between 0 to 1 using sigmoid-function according to

$$1 / (1 + e^{-I(S_j, S_i) + d}) \quad (7)$$

$$\text{where } d = \sum_{i=1}^n \sum_{j=1}^n \frac{I_1(S_j, S_i)}{n^2} \quad (8)$$

where n is model order, $I(S_j, S_i)$ is multivariate average mutual information $\{i, j = 1, 2, \dots, n\}$ and I_1 denotes values in multivariate AMI with delay of 1 sample.

In estimating time delay in the EEG signal and studying the flow of information in the brain average mutual information is proven to be a feasible method in analyzing epileptic seizures [Mars 1981]. The method has been applied to seizure localization using depth electrodes when epileptic focus was artificially created by electrical stimulation. The direction of the spread of activity determined by the computer and human EEGer coincided.

An example of EEG data in the beginning of the anaesthesia just after intubation (%-ET 2.0) is shown in figure 2 and corresponding correlated noise sources in figures

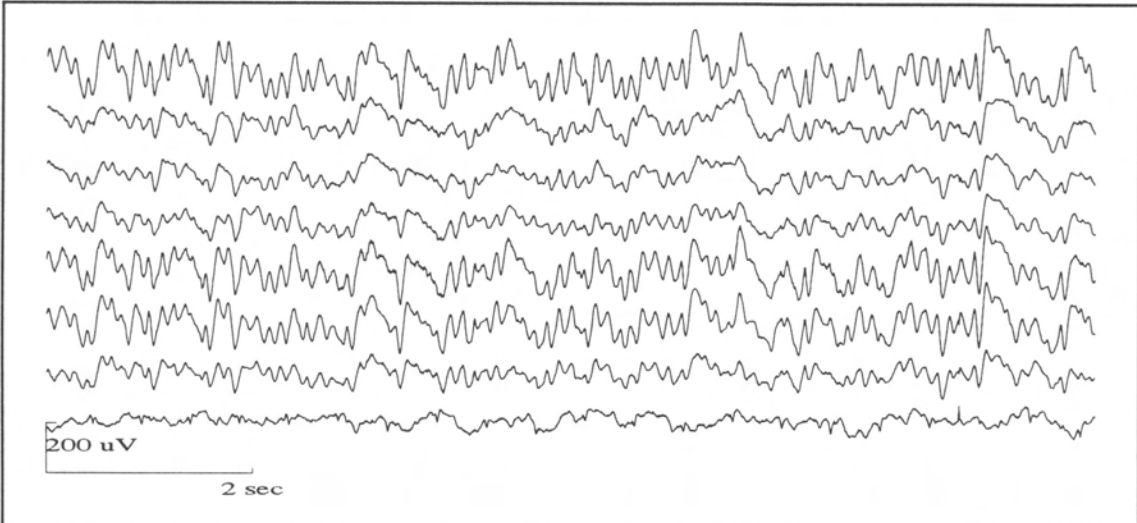


Figure 2. A example of EEG data in burst-suppression state; Cz-A1 (topmost), T6-A2, T5-A1, T4-A2, C4-A2, C3-A1, T3-A1 and A1-A2 (lowest).

3 and 4. The studied time delay T was 2 s and the order of closed-loop the MAR-model of 7 variables was 10. The analysis was performed with window size of 2048 samples i.e. corresponding to 10.24 s. The dotted line, in figures 3 and 4, between electrodes symbolizes the found correlated noise source between two measured EEG channels. The size of the circle in the middle of the line is determined according to the strength of the dependence between two channels. The size of circles are normalized so that the biggest value of correlated noise source is the same as the size of recording point circles (labelled as Cz, T3, etc.). All other statistically insignificant correlated noise sources are excluded.

Successive average mutual information based MAR-models were calculated to study variation in correlated noise sources during anaesthesia (figure 5). The analysis was performed for 11 min data using window size of 10.24 s with a step size of 10.24 s without overlapping. The selected channels for this study were: T6-A2 to T5-A1, C4-A2 to C3-A1, T4-A2 to T3-A1, T4-A2 to T5-A1, T4-A2 to C3-A1 and T4-A2 to Cz-A1.

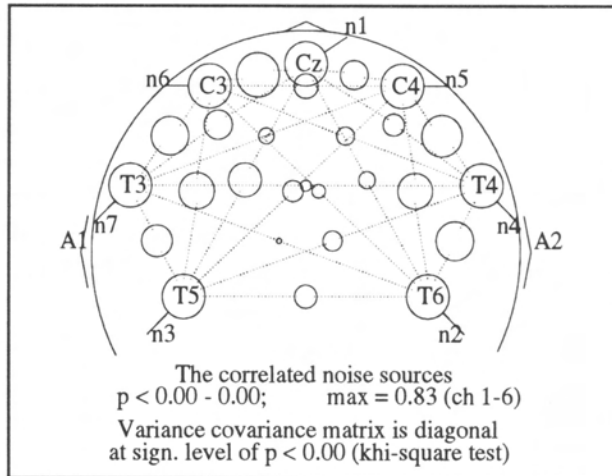


Figure 3. Calculated correlated noise sources of EEG data, shown in fig 2, utilizing conventional correlation method.

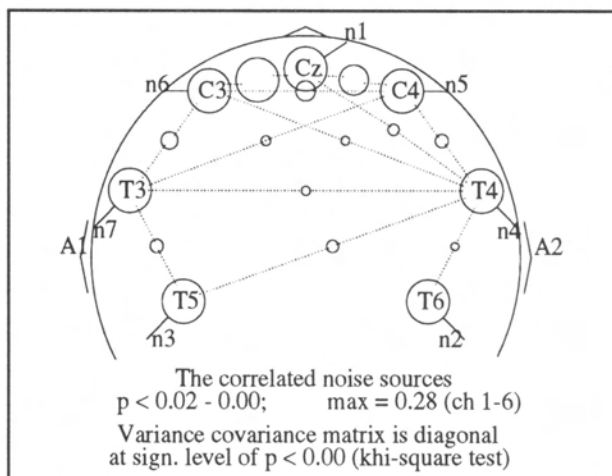


Figure 4. Calculated correlated noise sources of EEG data, shown in fig 2, utilizing average mutual information method.

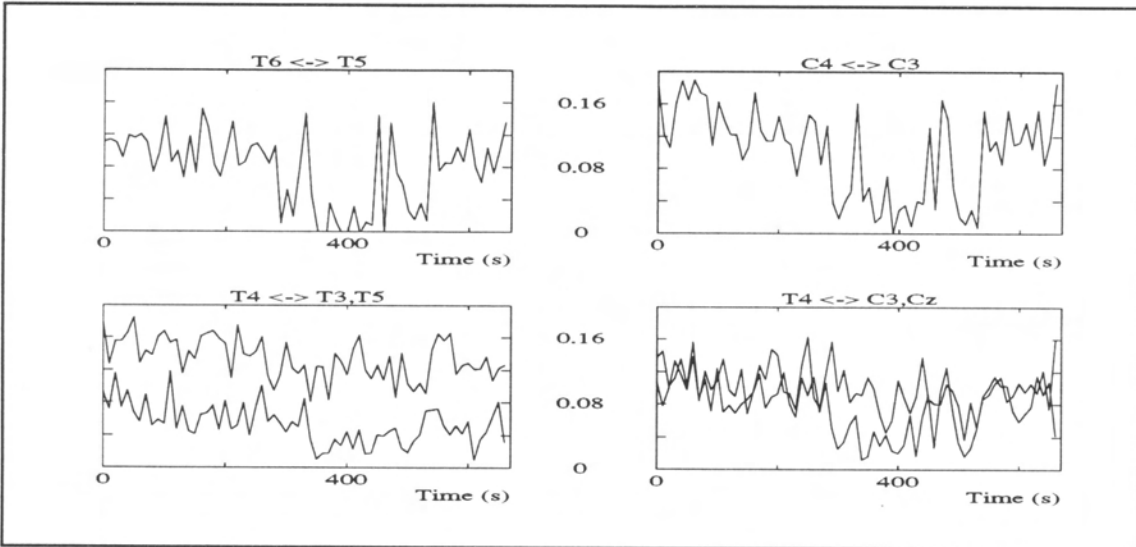


Figure 5. Changes in correlated noise sources between symmetrical channels during anaesthesia using average mutual information method. The recording contains burst-suppression activities around 400 sec.

CONCLUSIONS AND DISCUSSION

In the case of analyzing multichannel EEG time series with the MAR-model, there can be found noise sources, which effect several channels at the same time. In this case we can say that they have a common correlated noise source, which effect on them adding power to variables of MAR-model. Electrical activity potential fields inside the head are wide causing always some common activities in every EEG-channel, but certain differences in the power of the correlation between two channels can be differentiated from a normalized noise variance-covariance matrix. The statistically significant correlations between two channels may be very important in the analysis of flow of information or differentiating various activations mechanisms in the brain.

Because the MAR-model is sensitive in recognizing common activities between two channels, the possibility to find common correlated noise sources is bigger between measurements, which are physically located near each other. In an unipolar recording system the obtained correlated noise sources are very dependent on the reference electrodes, because it defines the direction of the measured activities. The detected result will be very different, if the reference electrode is ear, average reference or one of the other measurement point in 10-20 system i.e. bipolar recording. In our study the left (A1) or right ear (A2) reference electrodes were used. Using the ear reference the analysis results describe activities which are originated from large areas.

In general figures 3 and 4 demonstrate clearly the above described features. The results noticed, in figure 3, indicate a significant correlation between all measurement points, but the strongest correlated noise sources are between recording locations which have the same reference electrode or are located near each other - as expected. The particularly interesting property, in figure 4, is the fact that the correlated noise sources are found between distant recording locations around T4 and C4 indicating the presence of an activity source in the brain near recording location T4. Other interesting non-linear correlated noise sources can be distinguished around T5 and T3 revealing

common activities connected to the recording places T4 and C4. Underlining the above described results the non-linear based MAR-model seems to expose surprisingly well the distant interactions in the brain. Other noticeable difference in the built MAR-models is the average level of the variance covariance matrix. The variance covariance matrix, which is determined on the basis of the conventional correlation method contains bigger values (max. 0.83) than average mutual information dependent variance covariance matrix (max 0.28). Thus we can conclude that the correlation method is the optimal method for linearly correlated noise sources, but AMI-method may reveal nonlinear connections between EEG signals, which are not readily seen in linear model.

First, figure 5 demonstrates very clearly the gradual decrease in the values of correlated noise sources until the burst-suppression pattern appears in the EEG around time 400 s. In the low-activity suppression state there are not any correlated noise sources. On the contrary, the correlated noise sources in burst state are even bigger than before burst-suppression state. After burst-suppression the anaesthesia is lightened and the increasing trend is noticed. Based on these observations we can assume that the anaesthetic agents provoke systematical changes in the strength of the symmetrical dependence in EEG, which may be used, as a one indicator, to estimate the well-being of the brain during anaesthesia.

REFERENCES:

- Fraser A. and Swinney H. Independent coordinates for strange attractors from mutual information. Physical Review A, Vol 33; 2, Feb 1986, pp. 1134-1140.
- Gel'fand I. and Yaglom A. Calculation of the amount of information about a random function contained in another such function. Amer. Math. Soc. Trans. 1959, vol 12, pp. 199-246.
- Mars N. and Van Aragon G. Time delay estimation in nonlinear systems. IEEE Transactions on Acoustics, speech, and Signal Processing, Vol. ASSP-29; 3, June 1981, pp. 619-621.
- M. Priestley. Spectral analysis and time series. Vols 1 and 2, Academic Press, London, 1981.
- Shannon C. A mathematical theory of communication. Bell System Technical Journal. 1948, vol 27, pp. 379-423 & pp. 623-656.
- Shannon C. and Weaver W.. The mathematical theory of communication. University of Illinois Press, Urbana, 1949.

ABR Signal as a Digital Signal

Tapio K. Grönfors

Department of Computer Science and Applied Mathematics, University of Kuopio

INTRODUCTION

Auditory brainstem responses (ABR) are a sequence of electrical changes, generated in the brainstem and the central auditory pathways after the stimulation of the ears with various kinds of sounds. They are picked up with scalp electrodes by sensitive amplifiers and further processed by averagers. An ABR test performed on a subject can provide an objective measure of auditory nerve and brainstem dysfunction, even in the absence of clinical symptoms or signs. The ABR waveform is typically investigated in the time domain and the parameters of ABR are latencies and amplitudes of vertex positive response components which occur in an ABR signal. The response includes components I-VII of which I-V are usually investigated, V being the most important one [1,2].

In ABR experiments the stimulus is repeated typically 2000 times. For each repetition the response is represented in most systems either by 512 or 1024 sample points of the continuous analog signal sampled at fixed intervals. An ABR is the sum of a signal part, which is the same for each repetition, and a normally distributed noise part without mutual interference. The auditory brainstem potentials are weak signals (peak-to-peak amplitude is about 0.3 microvolts) and the noise is typically 10 or more times greater. The signal averaging is a very effective way to improve the signal-to-noise ratio, because the noise parts of different responses are assumed to be independent. The reduction in noise level depends on the randomness of noise and the number of repetitions made. For 2000 repetitions the reduction is by a factor of 45. Auditory brainstem responses are also very brief events. Therefore, their signal processing has to be executed really carefully.

ABR SIGNAL IN FREQUENCY DOMAIN

The power spectral analysis and the fast Fourier Transform (FFT) are traditional procedures for investigating the frequency composition of evoked potentials. Generally has been found that the information content of ABR is small above 2 kHz. Elberling has studied amplitude density spectra of ABR from normal material. Analyse have been performed on a high and low intensity ABR. In the spectral plot of a low intensity ABR there are clear peaks around 250 Hz and 500 Hz, and a high peak between 30-150 Hz. In the spectral plot of a high intensity ABR there are peaks around 500 Hz and 1kHz, and again a high peak between 30-150 Hz [3]. Doyle et al have compared the power density spectrum of a typical ABR recorded from normal material using click stimulation intensity of 70 dB nHL and the power density spectrum of a spontaneous EEG. In ABR spectra notches can be found over EEG spectra at 200 Hz, 500 Hz and just below 1 kHz [4]. Suzuki et al. have also used normal material, but pure tones instead of clicks. Generally in this study in the

power spectra of ABR there are peaks between 50-150 Hz, 500-600 Hz and just above 1 kHz [5]. Urbach et al. have somewhat different results, for in their power spectra of typical ABR, obtained by the periodogram method, the most prominent peak is between 240-480 Hz [6].

In our study of spectral analysis of ABR, due to the brevity of the digital ABR signal (only 512 points) we need special arrangements to calculate the power spectrum accurately with FFT to the ABR. At first, we remove the linear trend from a signal by computing a least squares fit of a straight line to the signal and subtracting the resulting function from the signal. This removes the DC component from the power spectrum. Next the 512 points discrete Fourier transform is performed by a radix-2 FFT algorithm. The power spectral density, a measurement of the energy at various frequencies, is calculated from FFT result. The frequency resolution is about 100 Hz. With the normal material (18 healthy subjects, median age 31 years) the most of the energy is concentrated between 450 and 800 Hz and quite lot of energy around 1000 Hz in a high intensity (80-90 dB nHL) click elicited recordings. In a lower intensity (60-70 dB nHL) ABR the energy around 1000 Hz is relatively reduced.

ABR DETECTION METHODS IN FREQUENCY DOMAIN

Some methods for analysis of ABR in frequency domain has been developed. Valdes-Sosa et al. have tested a statistical T2R method. T2R has been computed from the discrete Fourier transforms of 10 subaveraged ABR signals. At each frequency the distribution of the discrete Fourier transforms of the subaverages is complex normal with variance and mean. A measure for the presence of a signal at each frequency is the ratio of square of the sample estimate of mean to the sample estimate of variance. This ratio is close to zero in response absent condition and non-zero in response present condition. Dobie et al have used the magnitude-squared coherence (MSC) function an alternative to simple spectral analysis of auditory brainstem responses. It estimates the ratio of signal power to total power, varying from 0 to 1, for each frequency and thus indicates the degree to which an ABR is determined by the stimulus. The coherence function can be calculated on-line, and is computationally less complex than T2R test [7].

REFERENCES

1. Regan D. Human brain electrophysiology: evoked potentials and evoked magnetic fields in science and medicine. New York: Elsevier 1989.
2. Jewett DJ, Williston JS. Auditory-evoked far fields averaged from the scalp of humans. Brain 1971; 92: 681-96
3. Elberling C. Auditory electrophysiology: Spectral analysis of cochlear and brainstem evoked potentials, Scand Audiol 8 (1979) 57-64
4. Doyle DJ, Hyde M: Analogue and digital filtering of auditory brainstem responses, Scand Audiol 10 (1981) 81-9

5. Suzuki T, Sakabe N, Miyashita Y: Power spectral analysis of auditory brain stem responses to pure tone stimuli, Scand Audiol 11 (1982) 25-30
6. Urbach D, Pratt H: Application of finite impulse response digital filters to auditory brainstem evoked potentials, Electroenceph Clin Neurophysiol, 64 (1986) 269-73
7. Valdes-Sosa MJ, Bodes MA, Perez-Abalo M, Perera M, Carballo J, Valdes-Sosa P; Comparison of auditory evoked potential detection methods using signal detection theory, Audiology 26 (1987) 166-78

Signal Interpretation

Dynamical Aspects of Magnetic Source Imaging

S. J. Williamson

Department of Physics and Center for Neural Science
New York University, New York City, U.S.A.

This presentation will focus on several dynamical features of neural activity of the human brain that can be characterized by monitoring the accompanying magnetic field pattern just outside the scalp. The pattern of neural activity that is revealed by the analysis of magnetic field data is called a "magnetic source image" (MSI). The rapid response of magnetic sensors and the sharp spatial localization of neural sources provided by analyses of the field pattern make it possible to obtain information that has not been available by other techniques. In some cases is it possible to discriminate between simultaneously active regions of the brain that are separated by only a few centimeters distance. Another feature of MSI is the capability of providing a quantitative measure for the strength of neural activity, which is largely independent of the values of the conductivity of regions of the head that lie between the source and sensors. Two broad classes of brain activity will be considered: (1) Responses to sound stimuli and (2) Higher cognitive functions that are not temporally synchronized with an external time mark. MSI studies provide original contributions for the elucidation of dynamical features of both.

The first topic we shall address focuses on the well-known observation that a sensory stimulus such as an auditory tone presented at a periodic rate evokes a weaker signal from sensory areas of the brain if the time between stimuli is short. This feature clearly reveals a memory property. However, until recently little interest was generated by this phenomenon because, perhaps, researchers suspected that it was not a feature of the central nervous system. Instead, some argued that the weaker strength of neural activity when there are otherwise strong components (at 100 ms and 180 ms following the onset of a tone) may represent decreasing sensitivity of the peripheral sense receptors. Recent studies in our laboratory show that the effect can be classified technically as an example of habituation, and consequently it is a phenomenon of the central nervous system [1], not receptors in the ear.

There are four characteristics of habituation: (1) *decrement in amplitude* if stimuli are presented at a periodic rate with a short interstimulus interval; (2) *spontaneous recovery* of the amplitude if the stimuli are withheld for a short time; (3) *elevated response* to a probe stimulus that replaces a standard stimulus, thus indicating that the weak response is not due to an overall change in state of the brain; and (4) *dishabituation* whereby the insertion of a different stimulus between two standards causes an elevated response for the following standard. The last-named is the most crucial, since the effect is not expected if the receptors in the peripheral sense organ had become fatigued to the standard tone: The presentation of a different tone to which other receptors respond would have no effect on the fatigued receptor. In any event, researchers in our laboratory were able to demonstrate that responses in both primary and association cortices to auditory stimuli exhibit all four characteristics. Therefore, the weakening of the response amplitude as tones are presented at more rapid rates is

a central phenomenon. This indicates that a weaken response because of prior exposure to the same sound is evidence for a neural memory.

Because of the phenomenon of spontaneous recovery, studies of habituation for tone sequences presented at different interstimulus intervals provide a means for characterizing the lifetime of this neural memory. Remarkably, our studies of 4 subjects reveal that the neural memories associated with activity in the primary auditory cortex span a wide range, from about 0.8 to 3.4 s. It was critical for these studies to develop techniques to distinguish the magnetic field pattern of the primary auditory cortex from that of the association cortex, because their 100-ms components lie within 2 cm of each other [2]. Separate measurements of habituation in the association cortex showed the lifetime in each subject is 2 s longer than for primary cortex.

Behavioral studies on the individual subjects were carried out to determine how well these lifetimes agree with the length of time a person remembers features of a sound (known as "echoic" memory). Extensive measurements of the remembered loudness of a tone showed exponential relaxation to the mean loudness of all the sounds recently presented, thereby defining the lifetime for echoic memory. These values agree with those predicted by the previous "physiological" measurements obtained from magnetic source imaging [3]. This was the first time that a physiological study successfully predicted the duration of a memory. Such applications show the value of magnetic recordings, for the rapid response of the sensors is of critical importance for characterizing these dynamical changes.

Another topic that illustrates dynamical features of brain function is the well known presence of spontaneous rhythms of the cerebral cortex. Alpha rhythm in the bandwidth of 8 - 13 Hz is the best-known, and it can be detected without recourse to signal averaging. Our studies the field pattern of alpha rhythm over the posterior region of the scalp provide evidence that this rhythmic signal actually is comprised of discrete component parts [4]. While some researchers have emphasized that the amplitude distribution cannot be distinguished from narrow-band filtered white noise, our research clearly reveals the presence of short-term stability in the temporal and spatial features. Indeed, each short burst of alpha signal -- lasting for about 10 oscillations -- exhibits a remarkable period stability, and this period changes from one burst to the next. In fact, the period stability is significantly greater than can be accounted for by narrow-band filtered noise [5]. Moreover, the period abruptly changes as one burst follows another. The magnetic field pattern is also very stable during each burst, and abruptly changes as the succeeding burst becomes dominant. These observations indicate that occipital alpha rhythm may well be viewed as a sequence of cortical excitations (what we have called "alphons" [6]), each of which represents activation of a different patch of cortex.

MSI provides the capability to locate the cortical site of individual alphons. Of some interest is the fact that the spatial extent of each alphon is quite large for subjects who exhibit strong signals, so the strength of the source is correspondingly strong. Active cortical areas as great as 10 cm^2 for alphons were deduced when field patterns were explained in terms of sources of finite area [5]. However, in these cases the source strength per unit area of cortex is no greater than for ordinary sensory evoked responses. So we may tentatively conclude that individuals who exhibit strong alpha rhythm do not have an enhancement of the intrinsic strength but rather have a greater

correlation length across the cerebral cortex for their coherent rhythmic activity. Limited studies that we have carried out with a pair of 7-sensor neuromagnetometer probes reveal that the stronger alphas lie within the sulci that extend into the left and right hemisphere from the parietal and occipital regions of the longitudinal fissure. These correspond to regions of visual cortex.

Finally, we shall address the phenomenon of alpha suppression, when spontaneously activity is markedly attenuated over regions where the underlying cortical activity is participating in a sensory or cognitive process [7]. Studies in our laboratory have shown that the onset and offset of suppression measured magnetically provide significant measures for the duration of specific cognitive functions. In particular, investigations of visual imagery, silent rhyming, and short-term auditory working memory will be presented. The first two are variations of the same paradigm, whereby a word is displayed on a computer monitor and the subject was instructed to find an image of the object that the word represents, or in separate studies to find another word that rhymes with the displayed word [8]. The list of words is chosen so that in the latter case the word represents an abstract concept that is not easily represented by an image (for example the word *law*).

In both cases, there is immediate suppression of alpha over the visual cortex on presentation of the word. In the visualization paradigm, this suppression is continued for more than 1 s and is terminated at about the moment when the subject presses a reaction time key to indicate an image was found. Sometimes there is also suppression over the left anterior temporal and prefrontal areas. Subsequent interviews with subjects indicate that they occasionally talk to themselves when they try to find an image. That is a disadvantage of this particular paradigm.

By contrast, in the rhyming paradigm, alpha suppression over the visual area is maintained only for a few hundred milliseconds when the word is displayed. About 100 ms following visual presentation of the word, suppression commences over the left anterior temporal and prefrontal areas, but in this case it is maintained for 1 s or more and then is terminated about the time when the reaction time key is pressed to indicate that a rhyming word was found. Consequently, these studies of mental imagery and silent rhyming demonstrate that different areas of cortex participate in the two cognitive tasks, and they act at different time intervals. A interesting feature of the rhyming paradigm was observed for left-handed individuals, for some of them exhibit suppression over the right anterior temporal and prefrontal areas while others exhibit it over the left areas. This variation is not unexpected, since it is known that the dominant speech hemisphere may be on the right side for left-handed individuals.

New techniques of magnetic source imaging developed in our laboratory provide a way to deduce from field power measurements the underlying distribution of cortical current power, and by extension the distribution of where cortical current is suppressed [9]. This is based on the minimum-norm least-squares (MNLS) inverse, which is a mathematical procedure for deducing the pattern of transcortical current density from the field pattern measured across the scalp [10]. By comparing inverse solutions for average current power with and without suppression, it is possible to deduce specifically which areas of cortex exhibit suppression during complex cognitive tasks.

We may conclude from these examples that dynamical aspects of both sensory-related and spontaneous cortical activity can be characterized by MSI techniques where both the temporal and spatial information about the underlying source are important. These studies will become all the more powerful when large arrays of magnetic sensors are combined with methods to display the pattern of distributed cortical activity moment-by-moment.

REFERENCES

- 1) Z.-L. Lu, S.J. Williamson, and L.Kaufman. Human auditory primary and association cortex have differing lifetimes for activation traces. *Brain Res.*, 527:236--241, 1992.
- 2) S.J. Williamson, Z.-L. Lu, D. Karron, and L. Kaufman. Advantages and limitations of magnetic source imaging. *Brain Topography*, 4:169--180, 1991.
- 3) Z.-L. Lu, S.J. Williamson, and L. Kaufman. Physiological measurements predict the lifetime for human auditory memory of a tone. *Science*, 258:1668--1670, 1992.
- 4) Z.-L. Lu, J.-Z. Wang, and S. J. Williamson. Neuronal sources of parietooccipital alpha rhythm. In M. Hoke, S. N. Erné, Y. C. Okada, and G.-L. Romani, editors, *Biomagnetism: Clinical Aspects*, pages 33--37. Excerpta Medica, Elsevier, Amsterdam, 1992.
- 5) Z.-L. Lu, J.-Z. Wang, D. Karron, and S.J. Williamson. Support for the alphon hypothesis as a description of human alpha rhythm. In: *Proceedings of the 9th International Conference on Biomagnetism*, in press. 1994.
- 6) S.J. Williamson and L. Kaufman. Advances in neuromagnetic instrumentation and studies of spontaneous brain activity. *Brain Topography*, 2:129--139, 1989.
- 7) L. Kaufman, B. Schwartz, C. Salustri, and S. J. Williamson. Modulation of spontaneous brain activity during mental imagery. *J. Cog. Neurosci.*, 2:124--132, 1990.
- 8) L. Kaufman, Y. M. Cycowicz, M. Glanzer, and S.J. Williamson. Verbal and imaging tasks have different effects on spontaneous activity of cerebral cortex. *J. Exp. Psychol.: General*, in press, 1993.
- 9) J.-Z. Wang, L. Kaufman, and S. J. Williamson. Imaging regional changes in the spontaneous activity of the brain: An extension of the minimum-norm least-squares estimate. *Electroenceph. Clin. Neurophysiol.*, 86:36--50, 1993.
- 10) J.-Z. Wang, S.J. Williamson, and L. Kaufman. Magnetic source images determined by a lead-field analysis: The unique minimum-norm least-squares estimation. *IEEE Trans. Biomed. Engr.*, 39:665--675, 1992.

Event-Related Desynchronous Registration

Kalervo Suominen and Uolevi Tolonen
Dept. of Clinical Neurophysiology, Oulu University Central Hospital

The short-lasting amplitude attenuation or blocking of rhythmic activity within the alpha or beta bands before, during and after certain types of activation is called Event-Related Desynchronization (ERD). An event can be either a simple sensory stimulus, a motor action, or a complex cognitive task. EEG data is recorded and processed before, during and after such an event. ERD can be found in parallel to Event-Related Potentials (ERPs), e.g., visual stimulation results in the generation of VEP and changes in ongoing background activity.

MEASUREMENT AND QUANTIFICATION OF ERD

The scheme of ERD processing consists of EEG data sampling, bandpass filtering in the alpha band, squaring and averaging across all trials. In our system recording from 30 electrodes according to the international 10-20 system with additional electrodes between these standard positions is used. Reference electrodes are attached to earlobes and linked together. The patient is connected to a group of amplifiers and to a computer devoted to data acquisition. Signals are amplified with a 32 channels Braintronics EEG amplifier using 0.3 s time constant and 70 Hz upper frequency limit. The 7 seconds recording segment consists of pre-trigger (2 s) and post-trigger periods (5s).

The computer system for ERD recording consists of two PCs. A 16 MHz 80386SX is used for visual stimulation and data triggering and a 25 MHz 80386DX for data acquisition. The EEG is digitised at a sampling rate of 256 Hz and a voltage resolution of 12 bits with a Stellate Systems Rhythm software. The digitised EEG is stored on hard disk. In our laboratory the computers are linked together into a network, so we can move data to the file server and make data processing in a personal work station. The work stations are based on a 66 MHz 486 microprocessor with 8 Mbyte memory and a display resolution of 1280 x 1024 in a 20" multisync monitor.

The quantification of ERD is based on the averaging technique, each task is repeated 50 times. The alpha amplitude in the frequency band 8 - 12 Hz within the 7 sec segment is computed using digital linear phase, finite impulse response (FIR) filters and moving average method with 125 ms time window resulting power versus time curve. In order to obtain normalised measure of the ERD, a short EEG segment before the event occurs is defined as the reference interval. The average alpha power within this interval is the reference value. The ERD is then measured as a percentage alpha power decrease within the post-trigger interval and presented as a function of time.

DERIVATION AND ERD

In our system we are using reference-dependent recording, where reference electrodes are attached to earlobes and linked together. From this type of referential recording we can calculate reference-independent recordings such as bipolar derivation, common average, local average, weighted average reference derivation and Laplace derivation method.

In common average reference recording method the average of potentials recorded at each electrode at all times is subtracted from measured potentials. The weighted average and the local average derivations use weight functions, which depends on the interelectrode distances.

The Laplacian of the electric potential on the scalp surface is proportional to the current source density. The Laplace derivation method and local average reference derivation are in good agreement if the interelectrode distances are equal and the electrodes are positioned along perpendicular lines. Both methods give good source localisation, however, the quality of results deteriorates at the periphery, there are errors on the boundary electrodes.

CLINICAL ASPECTS

Until yet the measurement of ERD has been as a scientific tool. There are reports on its connection to e.g. memory, reading and motor performance. First clinical reports have shown that in TIA patients the attenuation of m-rhythm due to voluntary contraction of hand has been decreased on the affected site. In Parkinson's patients ERD due to hand clapping is weaker and occurs on larger area than in healthy controls. The measurement of ERD seems to be a promising potential tool for detection even mild disturbances of brain networks. The measurement of ERD is, however, technically demanding and time consuming and routine clinical use of this technique is still far away.

Patterns and Topology of Burst Suppression

Docent Ville Jäntti

Dept. of Clinical Neurophysiology, Tampere University Hospital
P.O.Box 2000 FIN-33521 Tampere, FINLAND

Burst suppression pattern in EEG has been known almost 60 years. In the paper where this phenomenon was first described by Derbyshire et al. (1936) they also studied the differences of this pattern in different regions of the cat brain as well as reactivity. Since then, however, no good, systematic studies on these aspects of the phenomenon have been done even though recording burst suppression pattern EEG are done with new anaesthetics when possible.

When seen after ischaemic brain damage, burst suppression is often an ominous sign. During anaesthesia it is, however, harmless and reversible. During recent years, anaesthesia at burst suppression level has been used in the treatment of intractable seizures, status epilepticus, and severe depression. During some surgical operations such as open heart surgery, burst suppression level anaesthesia has been claimed to protect the brain from ischaemia and attenuate the stress response.

Obviously, EEG monitoring equipment intended to be used during anaesthesia and in intensive care units should be able to correctly analyze burst suppression. In particular, the equipment should be able to make use of the different patterns, asymmetries, and other features of this phenomenon. Studying this pattern should also give important insight into the function of a damaged or intoxicated brain.

GENERAL

The burst suppression patterns caused by different anaesthetics are very different. Isoflurane produces mixed frequency bursts with rhythmic and arrhythmic components. Enflurane bursts may exhibit very sharp spikes, and the bursts can, in fact, develop into epileptic discharges. Recently we managed to record the enflurane-induced burst suppression of a dog, and the spikes in MEG were comparable with spikes recorded in epileptic discharges, as they are in EEG.

Suppression is not synonymous with isoelectricity. Isoflurane-induced suppression consists of low amplitude theta activity while enflurane suppression is very flat. During propofol-induced suppression 13 Hz spindles, exceeding 100 uV on the vertex, are seen. Previously, in fact, Scott, Binnie and Prior of St Bartholomew's Hospital, London, have used the name partial suppression to describe burst suppression after ischaemic brain damage, exhibiting relatively high amplitude mixed frequency activity during suppression. CFM and CFAM EEG monitors, developed by D. Maynard of Hatfield University U.K., have been designed to demonstrate these patterns, missed by most other EEG monitors. In 1985 Zaret reported alpha coma pattern during suppression.

Cortical EEG activity exists outside the frequency range used for monitoring. In the higher frequencies, somatosensory evoked potentials, for instance, can be recorded. At suppression onset the cortical potential drops to a very stable positive level. At burst onset it jumps to a slowly fluctuating (subdelta) negative level, on which the mixed frequency discharge appears. A similar step change in cortical potential is seen during generalized epileptic discharges. Propofol presents a burst onset very different from all the other anaesthetics we have used: the burst onset is slow, resulting in delta waves in a narrow bandpass recording. With isoflurane the step change reduces to a notch, which marks the end of suppression.

During continuous suppression, bursts can be evoked by minor tactile, sound or visual stimuli. In certain pathological conditions, a patient can actually be behaviorally awake when EEG shows this pattern. The pattern is, therefore, comparable with interictal epileptic discharges, which may have a very minor impact on the patient's behaviour.

TOPOGRAPHY AND PATTERNS

Isoflurane-induced bursts start with a burst of fast activity, maximum frontally. At the same time there is a step change of over 200 uV to a negative level, maximal at the central and occipital regions when using an extracerebral reference. The burst then develops into mixed frequency activity on rhythmic theta-delta activity, which gradually decreases in amplitude. In the end a step change to positive level is seen. If the recording is made with short derivations or transverse derivations the end of the burst may actually be difficult to detect. A short time constant reduces the step changes to notches, indicating the end of burst.

Propofol-induced bursts consist of mixed frequency activity and 13 Hz spindles. The negative DC shifts are lower in amplitude than with isoflurane and the shift in level is slower, resulting in slow waves rather than notches with short time constants. Spindles are also seen during suppressions: they are then on the negative side of the very stable positive suppression. The synchrony between hemispheres is remarkable.

PHYSIOLOGY

Little is known about the essentially nonlinear control system of burst suppression. It is not, however, limited to the cerebral cortex. Heart rate, for instance, is slightly depressed during suppressions, and this is vagally mediated.

SUMMARY

Burst suppression is readily produced by every healthy brain during general anaesthesia with many modern anaesthetics. Studying this phenomenon should give us insight in the function of the brain, including the mode of action of anaesthetic agents and the mechanisms responsible for limiting epileptic discharges. It is also essential in developing more advanced EEG monitoring techniques for anaesthesia.

Acknowledgements: The author is indebted to several colleagues, engineers and technicians: Arvi Yli-Hankala, Gerhard Baer, Michael Rorarius, Timo Porkkala, Päivi Annila, Seppo Mustola (anaesthesia), Pekka Loula, Alpo Värri, Tarmo Lipping, Kari Mäkelä, Kaisa Hartikainen (engineering), Mirja Uusitalo, Jaana Jurva, Jari Jurva (EEG technology), and several other persons who have supported the project.

FURTHER READING:

Derbyshire AJ, Rempel B, Forbes A and Lambert EF. The effects of anaesthetics on action potentials in the cerebral cortex of the cat. Amer. J. Physiol. 1936, 116: 557-596.

Jäntti V and Yli-Hankala A. Correlation of instantaneous heart rate and EEG suppression during enflurane anaesthesia: Synchronous inhibition of heart rate and cortical electrical activity? Electroenceph. clin. Neurophysiol., 1990, 76:476-479.

Jäntti V, Yli-Hankala A, Baer GA, Porkkala T. Slow Potentials of EEG Burst Suppression Pattern during Anaesthesia Acta Anaesthesiol Scand 1993; 37: 121 - 3

Jäntti V, Baer G, Yli-Hankala A, Hämäläinen M and Hari R. MEG burst suppression in an anaesthetized dog. Submitted.

Yli-Hankala A, Jäntti V, Pyykkö I and Lindgren L. Vibration stimulus induced EEG bursts in isoflurane anaesthesia. Electroenceph. clin. Neurophysiol. In press

EEG and ERP Dynamics in Slight Vigilance Variations

M.D. Hannu Mikola, Turku University Central Hospital

Electrophysiological Changes in Reduced Vigilance

Joel Hasan, M.D., Docent

Dept. of Clinical Neurophysiology, Tampere University Hospital
P.O.Box 2000 FIN-33521 Tampere, FINLAND

INTRODUCTION

Impaired performance due to excessive sleepiness and reduced vigilance is a serious problem in our present society. (Martikainen et al. 1992 & submitted). Polygraphy, including the electroencephalogram (EEG) the electro-oculogram (EOG) and submental electromyography (EMG) is considered to be one of the most reliable methods in order to assess whether a person is awake, drowsy or asleep (for references, see Santamaria and Chiappa 1987). An advantage is that the recordings interfere less with the vigilance of the subjects than psychological testing.

The rules of Rechtschaffen and Kales (1968) are almost exclusively used for sleep stage scoring and do not provide any means for the description of drowsiness without falling asleep or for any subdivision of "light" sleep. Although the electrophysiological changes related to drowsiness have been thoroughly studied (for references, see Hasan et al. 1993) to our knowledge nobody has tried to classify wakefulness and drowsiness into discrete levels by computer analysis and validated the results against human visual scoring. Even the attempts to classify wakefulness into discrete stages by human scoring alone are rare.

It is generally known that the electrophysiological changes related to drowsiness variate in a rapid manner. The epoch length of 20 or 30 s (Rechtschaffen and Kales 1968) which is used for whole-night recordings is thus too long for the description of rapid fluctuations of vigilance or short micro-sleep episodes.

In order to provide sensitive, and at the same time reliable, objective measures for the determination and quantification of reduced alertness, a computerized classification system has been under development in our laboratory. It includes a more detailed classification for the division of wakefulness and drowsiness into substages. The continuation of the epoch is determined by adaptive segmentation (Värtti 1988) producing short epochs of 0.5- 2 s. The length and content of the epochs are expected to correspond more closely to the real psychophysiological stages than by using a predetermined fixed epoch length.

In this presentation the methods so far developed by our group are described together with validation results obtained. Most of the studies have been done with: Kari Hirvonen and Veikko Häkkinen from the Tampere University Hospital, Alpo Värtti from the Tampere University of Technology, and Pekka Loula from the Technical Research Centre of Finland, Tampere. A brief description concerning topographical EEG studies together with Prof. Roger Broughton at the University of Ottawa will also be given.

RECORDING AND ANALYSIS

In our studies the EOG from two channels (Häkkinen et al. 1993), the EMG and the EEG from the derivations C3-A2 and P4-O2 are usually recorded and analysed. The signals are usually recorded on magnetic tape and later digitized off-line by using a 16-bit analog/digital converter with a sampling rate of 100 Hz. A PC/AT compatible computer with a 80386 processor, a 80387 numeric co-processor and a VGA monitor (resolution 640x480 pixels) is used for data acquisition, display, analysis and output. As a user interface, a previously developed computer software package, by which up to 8-channel recordings can be recorded, stored on disk, displayed and printed on paper was utilized (IMAPS, Loula 1991).

The recordings are automatically divided into segments of 0.5-2 s by adaptive segmentation on the basis of the amplitude and average frequency of the EEG signal recorded at the occipital (P4-O2) derivation (Värrí 1988). The segment boundaries are marked on screen and form the basis of later visual analysis. The average amplitudes of delta (0.5-2.0 Hz), theta (2.0-8.0 Hz), alpha (8.0-13.0 Hz), sigma (13.0-15.0 Hz) and beta (15.0-24.5 Hz) are calculated for each segment in both EEG channels using a doubly complementary filter bank. If the activity values of alpha and theta do not differ sufficiently in two consecutive segments of the two EEG channels, the segments are automatically combined. This results in longer segments, in practice seldom longer than 10 s.

The alpha activity measured at the P4-O2 derivation is given five symbolic levels depending on the amount obtained: 1. "low alpha", 2. "reference eyes open", 3. "intermediate", 4. "reference eyes closed" and 5. "increased". (Värrí et al. 1992). The theta activity recorded by the C3-A2 derivation is divided into three symbolic levels compared to the level measured during quiet wakefulness: 1. "decreased", 2. "reference" and 3. "increased".

The eye movements are distinguished from the EEG activity and many of the artifacts by requiring a negative correlation between the two recorded EOG channels in order to accept a detection by the computer algorithm (Värrí et al. 1990 & 1991). The EMs are classified into four categories: 1. blink, 2. saccade, 3. slow eye movement (SEM) and 4. other eye movement (OEM). The program most frequently classifies the rapid eye movements of REM sleep in category 2, occasionally in 1 or 4. The muscle tonus is quantified by filtering and integration. The symbolic representation of the EMG activity had three levels: 1. "decreased", 2. "reference" and 3. "increased". Each segment is visually classified into one of 7 stages: **WM**: movement and/or artifacts, **WO**: Alert, "eyes open" **WC**: Alert, "eyes closed", **D**: Drowsiness, **S1**: stage 1 sleep, **S2**: stage 2 sleep (including S3 and S4), and **SREM**: stage REM sleep.

The vigilance score of a segment was determined by a three-pass rule-based decision-making process. The number of if-then-else rules in the decision tree was 120. The leading principle in rule design was that the stage did not change unless clear features of a different state appeared. In the first pass only those segments considered to have unambiguous electrophysiological features for stage determination were scored. In the second pass the gaps left by the first pass were filled. During the third pass only a few refinements or corrections to the results of the first two passes are performed.

VALIDATION RESULTS

The first study presented is a validation study comprising 9 subjects undergoing a routine MSLT examination. In the validation the visual classification was performed independently by two preliminary and one consensus scorer. The agreements between the computer and visual scorings were relatively good for five subjects having a prominent occipital alpha activity during wakefulness (range 70-79 %) but less promising (range 64-70 %) for the other four subjects with "poor" occipital alpha activity. The values obtained corresponded to the inter-scorer agreements. Most of the discrepancies were between adjacent stages. At times in the presence of strongly fluctuating EEG amplitudes and especially with the "low-alpha" subjects it was very difficult to determine exactly even by visual scoring when, for instance, drowsiness became sleep.

The second study comprises examples of ambulatory recordings performed on 7 healthy male subjects. The results are somewhat better than in the former, the man/machine agreements being around 80 %. Examples of preliminary results from two other studies made on truck drivers in a simulator as well as drowsy patients with sleep apnea will also be given.

CONCLUSIONS

It is concluded that the reliability of the system is sufficient for practical purposes especially if critical parts of the recordings are visually reexamined. It was found to be difficult to define unambiguous scoring criteria for subjects with poorly defined EEG rhythms giving insufficient landmarks for stage determination.

QUANTITATIVE TOPOGRAPHIC EEG MAPPING DURING DROWSINESS AND SLEEP ONSET

The EEG of drowsiness and sleep has usually been recorded using a limited number of electrodes. Thus the spatial (topographical) distributions of the various EEG activities are largely undocumented. In the present study results from full scalp computerized topographical EEG analysis of both EEG transients and quantified EEG are reported. The main findings included: 1. Differences in frequency, distribution and temporal occurrence of the occipital alpha rhythm and other more diffuse alpha activities. 2. Presence of isolated anterior negative delta waves 3. Similarity between the vertex sharp waves and the saw-tooth waves in REM. 4. Distribution variability of spindle activity. 5. Gross insufficiency of a single central electrode. 6. Superiority of Cz electrode over parasagittal sites in the recording of transients and sleep spindles. The implications of similar and dissimilar field distributions and underlying brain source generators and psychophysiological functions are discussed.

REFERENCES

- Hasan, J., Hirvonen, K., Värri, A., Häkkinen, V. ja Loula, P. Validation of computer analysed polygraphic patterns during drowsiness and sleep onset. *Electroenceph. clin. Neurophysiol.* 87, 117-127, 1993.
- Hasan, J. and Broughton, R.J. Quantitative topographic EEG mapping during drowsiness and sleep onset. Accepted to: Proceedings of the symposium: Sleep Onset Mechanisms, Niagara-On-The-Lake, June 11-14, 1993, 20 pages.
- Häkkinen, V., Hirvonen, K., Hasan, J., Kataja, M., Värri, A., Loula, P. ja Eskola, H. The effect of small differences in electrode positions on EOG vigilance signals. *Electroenceph. clin. Neurophysiol.* 86, 294-300, 1993.
- Loula, P. Heart rate variation during anaesthesia and autonomic function tests. Licentiate thesis, Tampere University of Technology, Finland, 1991, 1-89.
- Hirvonen, K., Hasan, J., Häkkinen, V., Värri, A. and Loula, P. Automatic vigilance analysis & scoring system for ambulatory recordings. *Sleep Res.*, 20A: 496, 1991.
- Martikainen, K., Urponen, H., Partinen, M., Hasan, J., Vuori, I. Daytime sleepiness - a risk factor in community life. *Acta Neurol. Scand.* 86, 337-341, 1992.
- Martikainen, K., Partinen, M., Urponen, H., Vuori, I., Laippala, P. ja Hasan, J. Natural evolution of snoring: a 5-year follow-up study. Submitted to: *Acta Neurol. Scand.*
- Santamaria, J. and Chiappa K.H. The EEG of drowsiness. Demos Publications, NY 1987, 1-202.
- Värri, A. Digital processing of the EEG in epilepsy. Licentiate thesis, Tampere University of Technology, Finland, 1988, 67-70.
- Värri, A., Hasan, J., Hirvonen, K., Loula, P. ja Häkkinen, V. A computerized analysis system for drowsiness studies. *Comp. Meth. Progr. Biomed.* 39, 113-124, 1992.
- Värri, A., Häkkinen, V., Hasan, J. ja Loula, P. Eye movement detection for automatic vigilance analysis. In: *Sleep '90*. (Toim. J. Horne), s. 82-84, Pontenagel Press, Bochum, 1990.
- Värri, A., Häkkinen, V., Hasan, J., Loula, P. ja Hirvonen, K. A new nonlinear EOG processing method for vigilance analysis. Proceedings of the 1st European Conference on Biomedical Engineering, Nice, France, 17.-20.2.1991.

Appendix:

List of Symposium Participants

Lecturers

Prof. F.H. Lopes da Silva
University of Amsterdam
Faculty of Biology
Kruislaan 320
1098 SM AMSTERDAM
THE NETHERLANDS

Prof. Michael Scherg
University of Heidelberg
Schinkelstr. 37
D-80805 MÜNICH
DEUTCHLAND

Ph.D. Simon Walker
Tampere University of Technology
Ragnar Granit Institute
PL 692
33101 TAMPERE

Prof. Samuel Williamson
New York University/
Helsinki University of Technology
Low Temperature Laboratory
02150 ESPOO

M.Sc. Tapani Grönfors
University of Kuopio
PL 6
70211 KUOPIO

Prof. Riitta Hari
Helsinki University of Technology
Low Temperature Laboratory
02150 ESPOO

Docent Joel Hasan
Tampere University Hospital
Dept. of Clinical Neurophysiology
PL 2000
33521 TAMPERE

Dr.Tech. Matti Hämäläinen
Helsinki University of Technology
Low Temperature Laboratory
02150 ESPOO

Docent Ville Jäntti
Tampere University Hospital
Dept. of Clinical Neurophysiology
PL 2000
33521 TAMPERE

Lic.Tech. Pekka Loula
Technical Research Center of Finland
PL 316
33101 TAMPERE

Prof. Jaakko Malmivuo
Tampere University of Technology
Ragnar Granit Institute
PL 692
33101 TAMPERE

M.D. Hannu Mikola
Turku University Hospital
Dept. of Clinical Neurophysiology
Kiinanmyllynkatu 4-8
20520 TURKU

Dr.Tech. Riitta Salmelin
Helsinki University of Technology
Low Temperature Laboratory
02150 ESPOO

Docent Mikko Sams
Helsinki University of Technology
Low Temperature Laboratory
02150 ESPOO

M.Sc. Veikko Suihko
Tampere University of Technology
Ragnar Granit Institute
PL 692
33101 TAMPERE

Ph.D. Kalervo Suominen
Oulu University Hospital
Dept. of Clinical Neurophysiology
90220 OULU

Participants

Prof. Björn-Erik Erlandsson
University Hospital of Northern Sweden
Dept. of Biomedical Engineering
S-901 85 UMEÅ
SWEDEN

Engineer Lennart Gransberg
Karolinska Institute
Dept. of Clinical Neurophysiology
Box 130
S-171 76 STOCKHOLM
SVERIGE

M.D. Eric Hellstrand
Karolinska Institute
Dept. of Clinical Neurophysiology
Box 130
S-171 76 STOCKHOLM
SVERIGE

Biomedical Engineer Mikael Holub
University Hospital of Lund
Dept. of Clinical Neurophysiology
S-221 85 LUND
SVERIGE

Prof. Evert Knutsson
Karolinska Institute
Dept. of Clinical Neurophysiology
Box 130
S-171 76 STOCKHOLM
SVERIGE

Dr. Gunnar Larsson
National Center for Epilepsy
Pb 900
N-1301 SANVIKA
NORWAY

Research Engineer Eerik Lossman
Tallinn Technical University
Institute of Radio and
Telecommunication
Akadeemia tee 5
EE 0026 TALLINN
ESTONIA

Associate professor Ants Meister
Tallinn Technical University
Institute of Radio and
Telecommunication
Akadeemia tee 5
EE 0026 TALLINN
ESTONIA

Ph.D. Patricia Pardo
Helsinki University of Technology
Low Temperature Laboratory
02150 ESPOO

Ph.D. Heikki Teriö
University Hospital of Northern Sweden
Dept. of Biomedical Engineering
S-901 85 UMEÅ
SWEDEN

Prof. Claudia Tesche
Helsinki University of Technology
Low Temperature Laboratory
02150 ESPOO

Lic.Tech. Osmo Eerola
University of Turku
Centre of Cognitive Neuroscience
Electrocity
Tykistökatu 2-4
20520 TURKU

M.D. Nina Forss
Helsinki University of Technology
Low Temperature Laboratory
02150 ESPOO

Prof. Harry Frey
University of Tampere
Dept. of Clinical Medicine
PL 607
33101 TAMPERE

Prof. Gunnar Graeffe
Tampere University of Technology
Dept. of Electrical Engineering
PL 692
33101 TAMPERE

M.D. Marja-Liisa Granström
Childrens Castle Hospital
Lastenlinnanti 2
00250 HELSINKI

M.D. Riitta Heino
University of Turku
Dept. of Anesthesiology
Kiinanmyllynkatu 4-8
20520 TURKU

Ph.D. Erkki Heinonen
Helsinki University Central Hospital
Dept. of Clinical Neurophysiology
00029 HELSINKI

Ph.D. Juha Huttunen
Helsinki University Central Hospital
Dept. of Clinical Neurophysiology
00029 HELSINKI

M.D. Veikko Häkkinen
Tampere University Hospital
Dept. of Clinical Neurophysiology
PL 2000
33521 TAMPERE

Marketing manager, Neuromag
Juha Hämäläinen
Picker Nordstar, Inc
Elimäenkatu 24
00510 HELSINKI

M.Sc. Veikko Jousmäki
Helsinki University of Technology
Low Temperature Laboratory
02150 ESPOO

Assistant Jari Kaipio
University of Kuopio
Dept. of Applied Physics
PL 1627
70211 KUOPIO

Assistant Pasi Karjalainen
University of Kuopio
Dept. of Applied Physics
PL 1627
70211 KUOPIO

M.Sc. Jukka Kinnunen
Kuopio University Hospital
PL 21
70211 KUOPIO

Assistant prof. Leena Korpinen
Tampere University of Technology
Power Engineering
PL 692
33101 TAMPERE

Research assistant Antti Koski
University of Turku
Lemminkäisenkatu 14 A
20520 TURKU

Senior physician Johan Krause
Finnish Society for Medical Physics
and Medical Engineering
Kajaanintie 43
90210 OULU

M.Sc. Mika Kuusisto
University of Turku
Centre for Cognitive Neuroscience
Electrocity
Tykistökatu 2-4
20520 TURKU

M.D. Tero Kovala
Institute of Occupational Health
Topeliuksenkatu 41 a A
00250 HELSINKI

M.Sc. Mervi Könönen
Kuopio University Hospital
PL 21
70211 KUOPIO

Prof. Heikki Lang
Turku University Hospital
Dept. of Clinical Neurophysiology
20520 TURKU

M.Sc. Sari Levänen
Helsinki University of Technology
Low temperature Laboratory
02150 ESPOO

M.Sc. Tarmo Lipping
Tampere University of Technology
Signal Processing Laboratory
PL 553
33101 TAMPERE

Prof. Olli Lounasmaa
Helsinki University of Technology
Low Temperature Laboratory
02150 ESPOO

Proj. manager Kari Mäkihiemi
Instrumentarium Oy, Datex
PL 357
00101 HELSINKI

M.Sc. Tarja Niemi
Välikuja 2 C 10
21110 NAANTALI

M.D. Hely Oja
University of Tampere
Dept. of Biomedical Sciences
PL 607
33101 TAMPERE

M.Sc. Esa Ojala
Tampere University of Technology
Measurement Technology
PL 692
33101 TAMPERE

M.Sc. Matti Ollila
Friisiniityntie 15
02240 ESPOO

M.D. Ritva Paetau
Childrens Castle Hospital
Lastenlinnantie 2
00250 HELSINKI

Docent Juhani Partanen
Kuopio University Hospital
PL 21
70211 KUOPIO

Prof. Lauri Patomäki
University of Kuopio
Dept. of Applied Physics
PL 1627
70211 KUOPIO

Dr.Tech. Mauri Peltoranta
Finnyards Ltd Electronics
Naulakatu 3
33100 TAMPERE

Ph.D. Ari Pääkkönen
Kuopio University Hospital
PL 21
70211 KUOPIO

ECG-specialist Taisto Räsänen
Instrumentarium Oy, Datex
PL 357
00101 HELSINKI

M.D. Tapani Salmi
Helsinki University Central Hospital
Dept. of Clinical Neurophysiology
00029 HELSINKI

M.D. Stephan Salenius
Helsinki University of Technology
Low Temperature Laboratory
02150 ESPOO

Managing director Hannu Seitsonen
Kuulolaitekeskus Oy
PL 8
02101 ESPOO

M.D. Jouko Siivola
Kainuu Central Hospital
Dept. of Neurophysiology
87140 KAJAANI

M.Sc. Urpo Soukkanen
Tampere University Hospital
36280 PIKONLINNA

M.Sc. Pekka Tiihonen
Kuopio University Hospital
PL 21
70211 KUOPIO

M.Sc. Satu Tissari
Helsinki University of Technology
Low Temperature Laboratory
02150 ESPOO

Docent Uolevi Tolonen
Oulu University Hospital
Dept. of Clinical Neurophysiology
90220 OULU

M.D., Neurosurgeon Veijo Ukkola
Oulu University Hospital
Dept. of Neurosurgery
90220 OULU

Prof. Arto Uusitalo
Tampere University Hospital
Dept. of Clinical Physiology
PL 2000
33521 TAMPERE

M.D. Juha-Pekka Vasama
Helsinki University of Technology
Low Temperature Laboratory
02150 ESPOO

Dr. Tech. Alpo Värrä
Tampere University of Technology
Signal Processing Laboratory
PL 553
33101 TAMPERE

M.D. Ilkka Yletyinen
North Carelia Central Hospital
Dept. of Clinical Neurophysiology
80210 JOENSUU

Ragnar Granit Institute

Research Marko Anttila
Tampere University of Technology
Ragnar Granit Institute
PL 692
33101 TAMPERE

Docent Hannu Eskola
Tampere University of Technology
Ragnar Granit Institute
PL 692
33101 TAMPERE

Lic.Tech. Jari Hyttinen
Tampere University of Technology
Ragnar Granit Institute
PL 692
33101 TAMPERE

Research assistant Mika Isotalo
Tampere University of Technology
Ragnar Granit Institute
PL 692
33101 TAMPERE

M.Sc. Päivi Laarne
Tampere University of Technology
Ragnar Granit Institute
PL 692
33101 TAMPERE

Research assistant Kari Laukkanen
Tampere University of Technology
Ragnar Granit Institute
PL 692
33101 TAMPERE

M.Sc. Rami Lehtinen
Tampere University of Technology
Ragnar Granit Institute
PL 692
33101 TAMPERE

Secretary Soile Lönnqvist
Tampere University of Technology
Ragnar Granit Institute
PL 692
33101 TAMPERE

Research assistant Ari Haimilahti
Tampere University of Technology
Ragnar Granit Institute
PL 692
33101 TAMPERE

Dr.Tech. Juha Nousiainen
Tampere University of Technology
Ragnar Granit Institute
PL 692
33101 TAMPERE

M.D. Sakari Oja
Tampere University of Technology
Ragnar Granit Institute
PL 692
33101 TAMPERE

Technician Kari Puranen
Tampere University of Technology
Ragnar Granit Institute
PL 692
33101 TAMPERE

M.D. Ilpo Rimpiläinen
Tampere University of Technology
Ragnar Granit Institute
PL 692
33101 TAMPERE

Lic.Tech. Antti Rissanen
Tampere University of Technology
Ragnar Granit Institute
PL 692
33101 TAMPERE

Research assistant Rauno Roppo
Tampere University of Technology
Ragnar Granit Institute
PL 692
33101 TAMPERE

Research assistant James Rowland
Tampere University of Technology
Ragnar Granit Institute
PL 692
33101 TAMPERE

M.Sc. Kari Salminen
Tampere University of Technology
Ragnar Granit Institute
PL 692
33101 TAMPERE

M.Sc. Jari Viik
Tampere University of Technology
Ragnar Granit Institute
PL 692
33101 TAMPERE

**Ragnar Granit Institute
International Students**

Student Hamid Esmaeilpour Eslami
Tampere University of Technology
Ragnar Granit Institute
PL 692
33101 TAMPERE

Student Jafar Keshvari
Tampere University of Technology
Ragnar Granit Institute
PL 692
33101 TAMPERE

Student Jaanus Lass
Tampere University of Technology
Ragnar Granit Institute
PL 692
33101 TAMPERE

Student Aimur Raja
Tampere University of Technology
Ragnar Granit Institute
PL 692
33101 TAMPERE

Student Bing Tang
Tampere University of Technology
Ragnar Granit Institute
PL 692
33101 TAMPERE

Student Chengguo Cheng
Tampere University of Technology
Ragnar Granit Institute
PL 692
33101 TAMPERE

Student Toomas Värton
Tampere University of Technology
Ragnar Granit Institute
PL 692
33101 TAMPERE

Students

Student Tomi Alanen
Opiskelijankatu 9 A 24
33720 TAMPERE

Student Vesa Ekholt
Opiskelijankatu 4 C 175
33720 TAMPERE

Student Heta Haaslahti
Mekaniikanpolku 8 C 1
33720 TAMPERE

Student Jaana Hiltunen
University of Kuopio
Dept. of Applied Physics
PL 1627
70211 KUOPIO

Student Minna Huotilainen
University of Helsinki
Cognitive Psychophysiology Research
Unit
PL 11
00014 HELSINKI

Student Annukka Hyvärinen
Kivikartiontie 9 E 146
20720 TURKU

Student Matti Hämäläinen
Tampere University of Technology
Signal Processing Laboratory
PL 553
33101 TAMPERE

Student Timo Ikonen
Nuotiokatu 1 J 26
33580 TAMPERE

Student Juha Iso-Sipilä
Linnainmaanraitti 10 B 17
33580 TAMPERE

Student Kai Juottonen
Murkionkatu 4 A 16
20740 TURKU

Student Kirsi Juottonen
Murkionkatu 4 A 16
20740 TURKU

Student Tomi Kauppinen
Alatie 26
36200 KANGASALA

Student Petri Kiiski
University of Oulu
Dept. of Biophysics
PL 333
90571 OULU

Student Jukka Kivijärvi
Ollilantie 2 A as.4
37500 LEMPÄÄLÄ

Student Juha Kivitalo
Insinöörinkatu 60 D 243
33720 TAMPERE

Student Anu Koistinen
University of Kuopio
Dept. of Applied Physics
PL 1627
70211 KUOPIO

Student Ilmari Konka
Pellervonkatu 9 A 23
33540 TAMPERE

Student Jaana Korhonen
Opiskelijankatu 3 A 7
33720 TAMPERE

Student Marko Koski
Pinninkatu 16 B 40
33100 TAMPERE

Student Pekka Kumpulainen
Tampere University of Technology
Measurement Technology
PL 692
33101 TAMPERE

| | |
|-----------------------------------------------------------------------------------------------------------------------------|-----------------------------------------------------------------------------------------------------------------------------|
| Student Jorma Laaksonen University of Tampere Dept. of Clinical Medicine PL 607 33101 TAMPERE | Student Jari Sillanpää Insinöörinkatu 60 A 1 33720 TAMPERE |
| Student Juha Lavikainen University of Helsinki Cognitive Psychophysiology Research Unit PL 11 00014 HELSINKI | Student Janne Sinkkonen University of Helsinki Cognitive Psychophysiology Research Unit PL 11 00014 HELSINKI |
| Student Sami Mäkelä Itsenäisyydenkatu 18 B 18 33500 TAMPERE | Student Jari Taskinen Vaajakatu 5 B 25 33720 TAMPERE |
| Student Päivi Männistö Maalarintie 15 28800 PORI | Student Mika Tervonen Tampere University of Technology Signal Processing Laboratory PL 553 33101 TAMPERE |
| Student Mika Niemimäki Lapinkaari 1 33180 TAMPERE | Student Vesa-Pekka Torvinen Finninmäenkatu 4 N 124 33710 TAMPERE |
| Student Niko Paulanne Sorsapuisto 1 H 86 33500 TAMPERE | Student Mikko Uusitalo Helsinki University of Technology Low Temperature Laboratory 02150 ESPOO |
| Student Jari Puranen Insinöörinkatu 60 B 114 33720 TAMPERE | Student Kimmo Uutela Helsinki University of Technology Low Temperature Laboratory 02150 ESPOO |
| Student Katja Rajaniemi Opiskelijankatu 4 D 229 33720 TAMPERE | Student Ari Virtanen Opiskelijankatu 4 E 288 33720 TAMPERE |
| Student Marko Riihelä Finninmäenkatu 4 F 54 33710 TAMPERE | Student Petri Välimäki Insinöörinkatu 60 B 134 33720 TAMPERE |
| Student Elina Seitsonen University of Helsinki Faculty of Medicine Paraistentie 17 D 66 00280 HELSINKI | |

Ragnar Granit Institute

1992 VOL.6

- 1/1992 Karvonen, J., Honkanen, P. and Malmivuo, J.: Kokonais-hengitystyön mittaus
- 2/1992 Lönnqvist, S.: Annual Report 1991
- 3/1992 Suihko, V. and Eskola, H. (eds.): Proceedings of the First Ragnar Granit Symposium - Electrical and Magnetic Stimulation of Motor Nervous System, Tampere, Finland
- 4/1992 Eskola, H., Ahde, E. and Häkkinen, V.: Monopolar and dipolar modelling of the electro-oculography
- 5/1992 Harjunpää, R., Lehtinen, R. and Malmivuo, J.: EXES440-ohjelman EKG-parametrien poimintaohjelmisto
- 6/1992 Karvonen, J., Honkanen, P., Saari, M., Malmivuo, J. ja Uusitalo, A.: COPD:n vaikutus flowresistiiiveen kokonaishengityöhön

1993 VOL.7

- 1/1993 Lönnqvist, S.: Annual Report 1992
- 2/1993 Suihko, V., Malmivuo, J. and Eskola, H.: Sensitivity distribution of electrode leads in inhomogeneous spherical head model
- 3/1993 Savilahti, K. and Viik, J.: Coronary circulation in healthy and atherosclerotic patients. Description of angiography technique used in Tampere University Hospital
- 4/1993 Lahti, K.: An Overview of Intraventricular Impedance Imaging.
- 5/1993 Alahautala, T. and Lehtinen, R.: Computerized Recognition of the QT Interval from Exercise Electrocardiogram
- 6/1993 J. Hyttinen and J. Malmivuo (eds.): Proceedings of the Second Ragnar Granit Symposium: EEG and MEG Signal Analysis and Interpretation, November 22-23, 1993



P.O BOX 692, FIN-33101 Tampere, Finland
Tel. 931-316 2524, Telefax 931-316 2162